

## Spontaneous Article

# New description and diagnosis of *Eusthenodon wangsjoii* (Tetrapodomorpha, Tristichopteridae) from the Upper Devonian Britta Dal Formation of East Greenland

Jason P. DOWNS<sup>1,2\*</sup> 

<sup>1</sup> Department of Vertebrate Biology, Academy of Natural Sciences of Drexel University, 1900 Benjamin Franklin Parkway, Philadelphia, PA 19103, USA.

<sup>2</sup> Department of Biology, Delaware Valley University, Doylestown, PA 18901, USA.

\*Corresponding author. Email: [jason.downs@drexel.edu](mailto:jason.downs@drexel.edu)

**ABSTRACT:** In 1952, Erik Jarvik diagnosed and offered a brief description of the large-bodied, highly nested tristichopterid taxon *Eusthenodon*, and its type species *E. wangsjoii*, from fossils recovered from the Britta Dal Formation (Famennian) of Gauss Halvø (= Peninsula) and Ymer Ø (= Island) in East Greenland. The original diagnosis for *Eusthenodon* only needed to distinguish the tristichopterid taxon from the two others known at the time, *Eusthenopteron* and *Tristichopterus*, both of them small-bodied forms with anatomy now recognised to be primitive within the clade. Following that publication, no new large-bodied tristichopterids with *Eusthenodon*-like characteristics would be introduced until the description of *Mandageria fairfaxi* in 1997. In the 45 interim years, the limited descriptive details and insufficient diagnosis of *Eusthenodon* turned the name into a broadly applicable taxonomic label for large-bodied tristichopterid discoveries. Recent efforts to rediagnose the taxon and reconsider its global distribution of referred materials have improved the taxonomic utility of the name. However, no complete description of type species *E. wangsjoii* has yet been written. This is despite a type series of specimens that includes complete and articulated skulls that remain available for study in the collections of the Natural History Museum of Denmark (NHMD). The work presented here fulfils the need for a complete comparative description of *E. wangsjoii* in the context of the many highly nested tristichopterid species that have been described in the last three decades. New figures of the *E. wangsjoii* type series of specimens are the first to offer views of the fossils unobscured by the superimposition of interpretive line drawings. The new description is accompanied by a descriptive inventory of all the potential *E. wangsjoii* fossils at the NHMD and a new phylogenetic analysis of clade Tristichopteridae that includes revised character data for *E. wangsjoii* and adds one recently described species.



**KEY WORDS:** Famennian, Gauss Halvø, Palaeozoic, Sarcopterygii, tristichopterid, Ymer Ø.

*Eusthenodon* is a taxonomic group within Tristichopteridae, a cosmopolitan clade of extinct finned tetrapodomorphs from the Middle to Late Devonian Period (393–359 Ma). Before the recent descriptions of two species of *Eusthenodon* from the Catskill Formation (Duncannon Member, Famennian) of Lycoming County, Pennsylvania, USA (*Eusthenodon bourdoni* from Cogan House Exit Ramp, Downs *et al.* 2021, and *Eusthenodon leganihanne* from Trout Run, Downs *et al.* 2023), no enduring species had been assigned to this praenomen (= ‘genus’) since the 1952 description of the type species. Erik Jarvik (1952) coined the name *Eusthenodon* in his description of *E. wangsjoii*, a species (and praenomen) erected for fossils recovered from the Britta Dal Formation (Famennian) on Gauss Halvø (= Peninsula) and Ymer Ø (= Island), East Greenland. At the time of its description and diagnosis, *Eusthenodon* was only the third praenomen within Tristichopteridae (after *Tristichopterus* Egerton 1861; and *Eusthenopteron* Whiteaves 1881) and was the first to

exhibit a large body size (2.5 m, according to Jarvik’s 1952 body-length estimate) and the anatomical characteristics that are now recognised to be common among highly nested members of clade Tristichopteridae (including a teardrop-shaped pineal series in a caudal position; exclusion of jugal and postorbital from the orbital margin; a wide, recessed denticulated field of the parasphenoid; a caudal process of the vomer; a dentary fang pair; and an opercular that is taller than it is long; Downs *et al.* 2023). Many of the above listed features contributed to a diagnosis for *Eusthenodon* that has been invalidated in recent decades by the discovery of many additional highly nested tristichopterid species (13, according to the phylogenetic analysis of the present work) that share with *E. wangsjoii* some or all of these features (see Discussion in Downs *et al.* 2021).

The recent spate of descriptions and diagnoses that has expanded the alpha diversity of highly nested tristichopterids did not begin until the end of the 20th Century (none of the 13

additional highly nested species alluded to above were described before 1997, the year in which both *Cabonichthys burnsi* Ahlberg & Johanson 1997 and *Mandageria fairfaxi* Johanson & Ahlberg 1997 were introduced). Because Jarvik's (1952) original diagnosis for *Eusthenodon* only needed to distinguish the taxon relative to *Tristichopterus* and *Eusthenopteron*, until the diversity of highly nested tristichopterids became better understood in the 21st Century, '*Eusthenodon*' was used as a temporary taxonomic label for many undescribed fossil discoveries that represented a large-bodied tristichopterid with derived anatomy (see, e.g., Vorobyeva 1960; Thomson 1976; Lebedev 1992; Young 1993; Anderson *et al.* 1999; Ahlberg *et al.* 2001). This traditional use of the name resulted in *Eusthenodon* occurrences throughout Euramerica and Gondwana and a corresponding reputation for *Eusthenodon* as the one tristichopterid praenomen with a 'cosmopolitan' distribution (see Ahlberg *et al.* 2001, p. 9; Clément *et al.* 2009, p. 831). Downs *et al.* (2023) reviewed the entire history of *Eusthenodon* occurrences, within the modern context of known tristichopterid diversity, in an effort to clarify the known distribution of fossils that convincingly carry the *Eusthenodon* praenomen. This review supported reliable occurrences of *Eusthenodon* in only East Greenland and Pennsylvania, USA, but unsubstantiated additional reports of the taxon remain at Grenfell, New South Wales, Australia; in the Namur Province of Belgium; and in the Tula Region of Central Russia (*Eusthenodon*'s status as the sole cosmopolitan tristichopterid taxon has eroded further with the recent discovery of *Hyneria* in South Africa [Gess & Ahlberg 2023]). The historical review of *Eusthenodon* occurrences by Downs *et al.* (2023) relied on the revised diagnosis of *Eusthenodon* that was offered by Downs *et al.* (2021), the most substantial revision to the diagnosis since Jarvik's (1952) original.

Jarvik's (1952) diagnosis of *Eusthenodon* and type species *E. wangsjoii* consisted of 26 descriptive qualities of the type series of specimens. Downs *et al.* (2021) offered a character-by-character review of that diagnosis and the history of changes made to it in the decades subsequent. That review accompanied a description of *E. bourdoni*, the first of the two *Eusthenodon* species from the Catskill Formation of Pennsylvania that now share the *Eusthenodon* praenomen with the type species. Because of the limited taxonomic utility of the name *Eusthenodon*, for the reasons mentioned here and explained in full in the review of Downs *et al.* (2021), a major revision to the *Eusthenodon* diagnosis was required before the Pennsylvania fossils could be assigned to it. The revised diagnosis included only a combination of three features: a recessed denticulated field of the parasphenoid, an overlap of the squamosal onto the maxilla, and a marginal tooth row of the dentary that does not reach the symphysis. At the time, and through to the description of *E. leganihanne*, the species of *Eusthenodon* were the only tristichopterid species to exhibit this combination. The taxonomic status of *Eusthenodon* was improved by a diagnosis that not only distinguished the species of *Eusthenodon* among tristichopterids, but did so with discrete cranial features that are commonly preserved and not susceptible to interpretation and/or specimen deformation. However, even with the Downs *et al.* (2021) diagnosis for *Eusthenodon* (and the recent reviews of the praenomen's taxonomic history, Downs *et al.* 2021, and geographic occurrences, Downs *et al.* 2023), there remained no complete, comparative description for type species *E. wangsjoii*. Jarvik (1952, p. 56), not often terse in his descriptive writing, wrote that, '*Eusthenodon* in most respects agrees well with *Eusthenopteron* and other Osteolepiformes and a complete description will not be given'. This is despite the remarkable collection of complete and articulated cranial skeleton fossils from Greenland that Jarvik (1952) figured and that remain available for study (with revised catalogue numbers) in the collections of the Natural History Museum of Denmark (NHMD).

The comparative context of 1952 forced Jarvik to report on what are now recognised to be the broad differences between primitive and derived tristichopterid features, but there remains a need for a comparison between the condition in *E. wangsjoii* and in those of all subsequently described tristichopterids with derived anatomy and in highly nested phylogenetic positions. There is also a need for new figures to represent the anatomy of *E. wangsjoii*. Jarvik (1952) included 12 photographic plates in his original description, but he added interpretive line drawings directly onto the photographs that prevent the reader from independently assessing bone shapes, sizes and relationships. With six near-complete to complete articulated skulls among the 13 specimens in the type series alone (NHMD 141653, 141689, 141691, 141833 [holotype], 153855, 153925), *E. wangsjoii* may represent the single best opportunity to understand the cranial anatomy of a highly nested tristichopterid from a collection of high-quality fossils. Even without a complete description, *Eusthenodon* has long served as a model of derived tristichopterid anatomy.

*Eusthenodon* is a name with seven decades of use and no viable description; here I attempt to improve the taxonomic status of *Eusthenodon* and type species *E. wangsjoii* by providing a new, complete description of the type series of specimens, based on first-hand study and developed in the comparative context offered by all of those highly nested tristichopterid species described since 1952, including ones from Australia (*Cabonichthys burnsi* Ahlberg & Johanson 1997; *Edenopteron keithcrooki* Young *et al.* 2013; *Mandageria fairfaxi* Johanson & Ahlberg 1997), Belgium (*Langlieria socqueti* Clément *et al.* 2009) and the United States (*E. bourdoni* Downs *et al.* 2021; *E. leganihanne* Downs *et al.* 2023; *Hyneria lindae* Daeschler & Downs 2018; *Langlieria radiatus* [Newberry 1889]; *Langlieria smalingi* Downs & Daeschler 2022). A better resolved *E. wangsjoii* can support the assignment of new discoveries to the species and encourage the reassignment of specimens that have historically carried the name. I use the occasion of this *E. wangsjoii* redescription to also provide a descriptive inventory of all additional NHMD specimens that compare favourably with the anatomical condition in the species (see section 6.2). Finally, I offer a new phylogenetic analysis of Tristichopteridae, one that uses revised character data for *E. wangsjoii* and adds one new species that has been described since the cladistic consideration of Downs *et al.* (2023).

## 1. Geological and stratigraphic context

The *Eusthenodon wangsjoii* type series of specimens, as designated by Jarvik (1952), were collected during the Danish expeditions that Lauge Koch led to East Greenland between the years of 1929 and 1949. The holotype (NHMD 141833) and one paratype specimen (NHMD 153855) were collected at Sederholm Bjerg (= Mountain) on Gauss Halvø (Fig. 1a). The remaining paratypes were collected at Smith Woodward Bjerg (NHMD 141693), Kerstin Dal (= Valley; NHMD 141653, 153925), Paralleldal (NHMD 141689, 141691) and Remigolepisryg (NHMD 1201211) on Gauss Halvø, and at Celsius Bjerg (NHMD 141694, 1201204, 1201205, 1201222) and the southern shoreline of Dusén Fjord ('No. 162') on Ymer Ø (Fig. 1a). Decades later, Jarvik (1985) reported on and referred three additional specimens to *E. wangsjoii*. These had been collected in 1951 (NHMD 1201203 [P. 1636 of Jarvik 1985]) at Smith Woodward Bjerg on Gauss Halvø and in 1951 (NHMD 1201206 [P. 1693 of Jarvik 1985]) and 1955 (NHMD 1201216 [P. 1689 of Jarvik 1985]) at Celsius Bjerg on Ymer Ø. All of Jarvik's (1952, 1985) Gauss Halvø specimens are believed to be from the Britta Dal Formation (Famennian); all of those from Ymer Ø were collected at Celsius Bjerg, where the undifferentiated

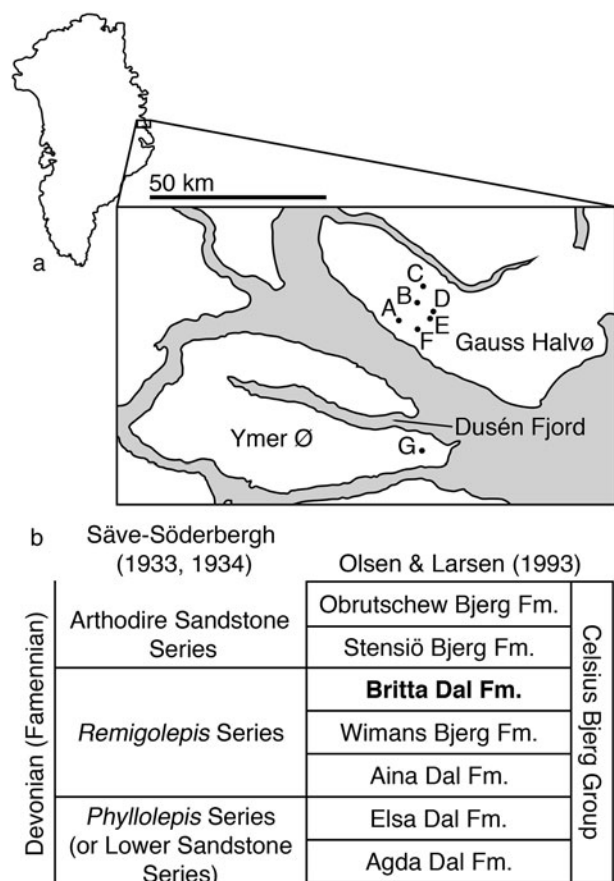


**Figure 1** (a) Map of Greenland (top left) and map of Gauss Halvø and Ymer Ø of East Greenland (inset image, modified from Jarvik 1996) showing the positions of the geological landmarks that were used in the original locality information for the described fossil specimens. All of the Gauss Halvø collecting sites are believed to be exposures of the Britta Dal Formation (Famennian). The labelled landmarks are (A) Smith Woodward Bjerg; (B) Paralleldal; (C), Sederholm Bjerg; (D), Remigolepisryg; (E), Kerstin Dal; (F) Stensiö Bjerg; and (G) Celsius Bjerg. (b) Correlation of the East Greenland Late Devonian (Famennian) stratigraphic schemes of Säve-Söderbergh (1933, 1934) and Olsen & Larsen (1993).

Famennian age strata prevent a precise stratigraphic assignment (Blom *et al.* 2007). The Britta Dal Formation, ~500 m thick at its maximum thickness along the southern coast of Gauss Halvø, comprises alternating siltstones and fine-grained sandstones (Olsen & Larsen 1993). The siltstones show symmetrical ripple marks and desiccation cracks; the sandstones show cross- and parallel lamination with lateral accretion bedding. Much of the formation is dark red but the dark red rock alternates with dark grey/green siltstones at 1–10 m scales in the upper part of the formation (Olsen & Larsen 1993). The facies of the Britta Dal Formation have supported an interpretation of floodplain (siltstones) and channel and point bar (sandstones) depositional settings along a meandering fluvial system (Olsen & Larsen 1993). The Britta Dal Formation belongs to the lithostratigraphic group that Olsen & Larsen (1993) named the Celsius Bjerg Group (Famennian), the uppermost of four groups defined in the work (the others, from lowest, are the Vilddal, Kap Kolthoff and Kap Graah Groups). All of the Celsius Bjerg formations represent freshwater depositional environments: lacustrine, alluvial mudflat, and fluvial channel and floodplain deposits; palaeocurrent direction is generally northward throughout the unit (Olsen & Larsen 1993).

Jarvik (1952) offered only the ‘Remigolepis Series’ as the geological context of the *E. wangsjoii* type series of specimens (Fig. 1b). The ‘Remigolepis Series’ was the middle of the three

biostratigraphic units established by Säve-Söderbergh (1933, 1934) to divide the Late Devonian stratigraphic succession of East Greenland (the other two are the ‘Phyllolepis Series’ [‘Lower Sandstone Complex’ of Säve-Söderbergh 1933] below and the ‘Arthodire Sandstone Series’ above). The ‘Remigolepis Series’ was recognised by a particular faunal assemblage that commonly included the species of *Remigolepis*, but it was also the only East Greenland assemblage to yield limbed tetrapodomorphs. According to Olsen & Larsen’s (1993) lithostratigraphic revision of East Greenland’s Devonian sediments (Fig. 1b), the ‘Remigolepis Series’ equates to the Aina Dal, Wimans Bjerg and Britta Dal Formations of the Celsius Bjerg Group (Famennian). The Britta Dal is the fifth formation in the seven-formation sequence that comprises the Celsius Bjerg Group (Agda Dal and Elsa Dal, the lowest two; Stensiö Bjerg and Oubrutschew Bjerg the upper two; Olsen & Larsen 1993). In addition to *E. wangsjoii*, the vertebrate fauna of the Britta Dal Formation (Blom *et al.* 2007) includes the dipnoans *Jarvikia arctica* Lehman 1959 and *Oervigia nordica* Lehman 1959; the limbed tetrapodomorphs *Acanthostega gunnari* Jarvik 1952, *Ichthyostega watsoni* Säve-Söderbergh 1932 and *Ichthyostega eigili* Säve-Söderbergh 1932; and the antiarchs *Remigolepis acuta* Stensiö 1931 and *Remigolepis incisa* (Woodward 1900).

## 2. Materials and methods

### 2.1. Rationale for selecting specimens upon which to base the description

No complete description of *Eusthenodon wangsjoii* has yet been written. I propose reasons for this in the introduction above; importantly, insufficient anatomical representation among the type series of specimens is not one of these reasons. The description of the species provided by the present work is strictly based upon 11 of the 13 specimens in the *E. wangsjoii* type series as designated by Jarvik’s (1952) original reporting (see referred materials in section 3). The two paratype specimens that are not considered in this new description are, first, the isolated scale that Jarvik (1952) designated as ‘No. 162’ (following the convention established by Stensiö 1931 in his reporting on the same specimen) from locality 3 (of Stensiö 1931, text-fig. 1), south of Dusén Fjord, Ymer Ø, and, second, NHMD 153855 (P. 1473 of Jarvik 1952), a complete skull from Sederholm Bjerg, Gauss Halvø, East Greenland. The first of these two specimens, ‘No. 162’, is an isolated scale that is not currently identifiable in the NHMD collection and therefore has not been given a modern NHMD specimen number and is not available for study (B. E. K. Lindow, pers. comm., 2023). Even if the specimen was available, because it is an isolated scale unassociated with *E. wangsjoii* cranial material (indeed any cranial material according to Stensiö 1931), I would not have used it as the basis for the *E. wangsjoii* scale description provided here. I chose instead only scales associated with (and sharing specimen numbers with) the skull material in the *E. wangsjoii* type series. The second of the paratype specimens not considered in the new species description is a skull (NHMD 153855) that may indeed represent *E. wangsjoii*, but, if it does, it does so as a juvenile individual due to the considerable size and shape differences between it and the other specimens in the type series. The total length of the skull roof in NHMD 153855 is 8.28 cm; compare this to the same length in the holotype (17.97 cm in NHMD 141833), itself small relative to, for example, paratype specimen NHMD 153925 (wherein the parietal shield alone is ~20.81 cm in length). This small skull is described here, along with all other potential *E. wangsjoii* fossils in the NHMD collection, but only in a separate section (6.2) away from the species description.

Because ‘*Eusthenodon*’ and indeed ‘*Eusthenodon wangsjoii*’ spent decades as the only appropriate labels for large-bodied tristichopterid fossils exhibiting derived anatomy, an attempt to base a new description for the species on all referred materials worldwide is unfeasible. But there is also reason not to base the new description on all of the fossils from the Britta Dal Formation that have been identified as ‘*Eusthenodon*’, or even just those that are from the Britta Dal, labelled ‘*Eusthenodon*’, and within the collections at the NHMD. Many of those NHMD fossils that have carried the name ‘*Eusthenodon* sp.’ or ‘*Eusthenodon wangsjoii*’ only did so because they appear consistent with the expectations of derived tristichopterid anatomy and have therefore historically fallen under the broad umbrella implied by an insufficient diagnosis for *Eusthenodon*. My recent work in the NHMD collections revealed the strong likelihood of at least one additional tristichopterid species from the Britta Dal Formation, which calls further into question the assignment of many of these partial or fragmentary fossils currently carrying a ‘*Eusthenodon*’ label. In addition, some of these fossils (including the three later referred to *E. wangsjoii* by Jarvik (1985) himself: NHMD 1201203, 1201206 and 1201216) show conditions that are counter to those consistently exhibited by the fossils in the type series.

In addition to providing a complete comparative description of *E. wangsjoii* (section 4) based upon the original type series of specimens (excepting ‘No. 162’ and NHMD 153855 for the reasons stated above), the present work also includes brief descriptions of all the potential *E. wangsjoii* specimens in the NHMD collection (section 6.2). These specimens (with the exception of NHMD 153855 [paratype]), with suggestive anatomy but outside the type series, are here assigned to cf. *E. wangsjoii*. Sections 4 and 6.2 of the present work, then, present the entirety of the NHMD collection that is relevant, or even potentially relevant, to a new understanding of *Eusthenodon* and its type species *E. wangsjoii*.

## 2.2. Phylogenetic analysis

The species-scale phylogenetic analysis presented in this work was conducted on an in-group of 19 species, adding one to the data matrix compiled for the analysis of Downs *et al.* (2023). The new addition is *Hyneria udlezinye*, recently described from the Witpoort Formation at Waterloo Farm, Makhanda, South Africa, by Gess & Ahlberg (2023). Many of the character data used here were compiled to support the analyses of Ahlberg & Johanson (1997, 1998), Snitting (2008), Clément *et al.* (2009), Downs & Daeschler (2022) and Downs *et al.* (2023). Olive *et al.* (2020) used 20 characters from historical analyses and added six (nos. 21–26); Downs & Daeschler (2022) added an additional one (no. 27). That list of 27 characters is used here, and most character scores specifically reflect those recorded, revised or retained by Downs *et al.* (2023). Since the analysis of Downs *et al.* (2023), I revised 13 character scores, seven of which belong to *E. wangsjoii*; explanations and specimen support for those revisions is compiled in supplementary File 1 available at <https://doi.org/10.1017/tre2500001>. I also renumbered the character states of character 26 to eliminate the character state (former state 1) not observed among known tristichopterids and added a new character state (new state 2) to better reflect the condition in *Cabonnichthys burnsi*.

I built the data matrix (supplementary File 2 and available at Morphobank: <http://morphobank.org/permalink/?P5678>) in Mesquite version 3.70 (build 940; Maddison & Maddison 2021) and analysed it using the branch-and-bound search algorithm of PAUP 4.0a169 (Swofford 2002; supplementary File 3). Characters 4, 24, 26 and 27 are multi-state characters; all characters were given equal weight and all character states were treated as unordered. Like the analyses of Downs &

Daeschler (2022) and Downs *et al.* (2023), I used *Gogonasmus andrewsae* and *Spodichthys buetleri* as out-groups due to the completeness of their character data and the historical support for their phylogenetic proximity to Tristichopteridae (e.g., Ahlberg & Johanson 1998; Zhu & Ahlberg 2004; Snitting 2008; Swartz 2012). Tree length (L) and consistency, retention and rescaled consistency indices (CI, RI, RCI) of the most parsimonious trees were calculated in PAUP. PAUP was also used to generate a strict (SCT) and a 50% majority-rule consensus tree (MRCT) from all of the most parsimonious trees (MPTs); to calculate CI, RI and RCI of the consensus trees; to calculate Bremer support values for the nodes of the strict consensus tree; and to resolve the positions of the character state transitions on the consensus trees.

## 2.3. Institutional abbreviations

AMF, Australian Museum, Sydney, Australia; ANU V, Australian National University, Canberra, Australia; ANSP, Academy of the Natural Sciences of Drexel University, Philadelphia, USA; CPC, Commonwealth Paleontological Collection, Bureau of Mineral Resources, Canberra, Australia; NHMD, P, Natural History Museum of Denmark, Copenhagen, Denmark.

## 3. Systematic palaeontology

Sarcopterygii Romer 1955  
Osteolepiformes Berg 1937  
Tristichopteridae Cope 1889

**Diagnosis.** Osteolepiform sarcopterygians with postspiracular bone present, vomer with long caudal process clasping the parasphenoid, circular scales with a median boss, and an elongate body with trifurcate tail (Ahlberg & Johanson 1997).

*Eusthenodon* Jarvik 1952

**Etymology.** From the Greek *eû*, good; *sthénos*, strength; and *odôn*, tooth; in reference to ‘the large and stout tusks in the upper and lower jaws’ (Jarvik 1952, p. 54).

**Type species.** *Eusthenodon wangsjoii* Jarvik 1952

**Revised diagnosis.** Tristichopterid distinguished by the combination of (1) a denticulated field of the parasphenoid that is recessed into the body of the bone, (2) a marginal tooth row of the dentary that does not reach the symphysis and (3) a scale ornament comprising conjoined tubercles and straight to sinuous ridges (modified from Downs *et al.* 2021).

**Comments.** *Eusthenodon* is a praenomen of Famennian tristichopterid tetrapodomorphs that presently includes three species: the type species *E. wangsjoii* Jarvik 1952; *E. bourdoni* Downs *et al.* 2021; and *E. leganihanne* Downs *et al.* 2023. The most recent published diagnosis for *Eusthenodon* (Downs *et al.* 2021) was a combination of three features, the first two of which are retained in the revised diagnosis presented here: a denticulated field of the parasphenoid that is recessed into the body of the bone, a marginal tooth row of the dentary that does not reach the symphysis, and a squamosal that overlaps the maxilla. Within *E. wangsjoii*, the best support for the inclusion of the third feature was NHMD 1201206, an isolated dermal impression of a maxilla from Celsius Bjerg that Jarvik (1985) assigned to the species but is here removed from consideration in the species description (see section 2.1). Among the holotype and paratype specimens of *E. wangsjoii*, the overlapping relationship between maxilla and squamosal is the opposite condition (maxilla overlaps squamosal; see NHMD 1201204), a condition that is even counter to the condition in both other species of *Eusthenodon* (Downs *et al.* 2021, 2023). Removing that feature from the *Eusthenodon* diagnosis leaves a combination of only two features that applies (or may apply) to several other species of tristichopterid. *Edenopteron keithcrooki* exhibits both of these remaining features (Young *et al.* 2013, 2019); *Langlieria smalingi* and

*Hyneria udlezinye* exhibit a dentary tooth row that does not reach the symphysis and the condition of the parasphenoid's denticulated tooth plate is unknown (Downs *et al.* 2021; Gess & Ahlberg 2023). In order to present a diagnosis for *Eusthenodon* that exclusively applies to the three species that presently carry the praenomen, a particular scale ornament (of conjoined tubercles and straight to sinuous ridges) is added to the combination, one that is observed in all three species and is unlike that of *E. keitherooki* and *L. smalingi* (where scale surface is smooth and with incised grooves; Young *et al.* 2013; Downs *et al.* 2021, 2023; Downs & Daeschler 2022).

*Eusthenodon wangsjo* Jarvik 1952

**Etymology.** Named after palaeontologist Dr Erik Gustav Albin Wängsjö (1909–1985) of Östergötland County, Sweden, to honour his having collected many of the specimens in the type series (Jarvik 1952).

**Holotype.** NHMD 141833 (P. 1476 of Jarvik 1952; Fig. 2), nearly complete skull, much of it preserved in dermal impression, including skull roof and extrascapulars, left and right cheeks, left and right lower jaws and principal gulars, and left submandibulars.

**Type locality and horizon.** 1,174 m. horizon (Britta Dal Formation, Famennian) at Sederholm Bjerg, Gauss Halvø, East Greenland.

**Referred materials.** NHMD 141653 (P. 1479 of Jarvik 1952; Fig. 3), skull, partial left lower jaw and pectoral fin bones; 141689 (P. 1477 of Jarvik 1952; Fig. 4), partial parietal shield, right cheek and scales; 141691 (P. 1478 of Jarvik 1952; Fig. 5), skull; 141693 (P. 1483 of Jarvik 1952; Fig. 6), right lower jaw, submandibulars and principal gular; 141694 (P. 1481 of Jarvik 1952; Fig. 7), right opercular, cleithrum and pectoral fin bones; 153925 (P. 1480 of Jarvik 1952; Fig. 8), skull and lower jaws; 1201204 (P. 1474 of Jarvik 1952; Fig. 9), partial right cheek and infradentary; 1201211 (P. 1482 of Jarvik 1952; Fig. 11), parasphenoid [impression]; and 1201222 (no. 101 of Jarvik 1952; Fig. 12), partial parietal shield.

**Diagnosis.** Tristichopterid referred to *Eusthenodon* and distinguished from *Eusthenodon bourdoni* and *Eusthenodon leganihanne* by a maxilla that overlaps the squamosal.

**Comments.** The redescription of *E. wangsjo* presents an opportunity to diagnose the type species relative to the other species that share the praenomen. *Eusthenodon wangsjo* is the only species of *Eusthenodon* that shows maxilla overlap onto the squamosal and so the relationship is sufficient justification for assigning *Eusthenodon* fossils to the type species. The presence of at least two pitline grooves on the squamosal also distinguishes *E. wangsjo* from the known conditions in the two other species of *Eusthenodon*, but because the condition is unknown in *E. leganihanne*, the feature is not included in the *E. wangsjo* diagnosis presented here.

## 4. Description

### 4.1. Dermatocranial dimensions, ornament and pitline grooves

The parietal shield of *Eusthenodon wangsjo* is long relative to the length of the postparietal shield and wide relative to its own length. The midline length ratio of parietal shield to postparietal shield is 2.29 in the *E. wangsjo* holotype (NHMD 141833) and between 2.06 and 2.29 when considering the two specimens that allow for this measurement (NHMD 141691 the other). This minimum range of the ratio in *E. wangsjo* approximates the conditions in both other species of *Eusthenodon*: *Eusthenodon bourdoni* (same ratio is 2.15 in the single complete skull roof specimen, ANSP 23748A, Downs *et al.* 2021) and *Eusthenodon*

*leganihanne* (~2.0 in the single complete skull roof specimen, ANSP 21343). A long parietal shield relative to postparietal shield is common among the few highly nested tristichopterid species for which the calculation is possible. These additionally include *Cabonnichthys burnsi* (~2.2 in AMF 96856A, Ahlberg & Johanson 1997) and *Mandageria fairfaxi* (2.1, as reported by Johanson & Ahlberg 1997).

The width/length ratio of the parietal shield of *E. wangsjo* (when width is maximum width measured across the anterior supraorbital bones) is between 0.49 and 0.56 based on the two specimens that allow for measurement (NHMD 141691 [0.49, width extrapolated from right side preservation], 153925 [0.56]). This minimum range for the ratio makes for the wide skull and blunt snout that is typical for species of *Eusthenodon* and indeed for many of the highly nested species of Tristichopteridae, with the notable exception of *M. fairfaxi* (same ratio is ~0.38 in F96508; Johanson & Ahlberg 1997), a species that is partly diagnosed by its narrow and pointed skull roof. The width/length ratio of the parietal shield in both other species of *Eusthenodon* is within the range of values observed in *E. wangsjo*; only one specimen of *E. bourdoni* (0.55 in ANSP 23748) and one specimen of *E. leganihanne* (0.51 in ANSP 21343) allow for the calculation.

The postparietal shield of *E. wangsjo* is wider than long. Though the maximum postparietal shield width/length ratio among the study specimens (1.95) is in the largest postparietal shield (NHMD 1201205, largest in both midline length and maximum width), the ratios in *E. wangsjo* do not trend with either the shield's midline length or its maximum width. The values range between 1.29 and 1.95 for the four postparietal shield specimens used as the basis for this description (the others are NHMD 141653 [1.73, width extrapolated from right side preservation], 141691 [~1.50] and 141833 [1.29, width extrapolated from right side preservation]). Jarvik (1952) cited the ratio of 1.70 in his description of *E. wangsjo*, a value that seems likely to have been measured from NHMD 153855 (then P. 1473; ratio = 1.71), a specimen that is here assigned to cf. *E. wangsjo* (see section 2.1) and described in section 6.2. Johanson & Ahlberg (1997) cited a ratio of 1.75 for the species, a value that is at the wider end of the range presented here. The value of the width/length ratios in the two other species of *Eusthenodon* fall within the range measured for *E. wangsjo* (1.67 in the one complete specimen of *E. bourdoni*, ANSP 23748, Downs *et al.* 2021; and 1.59 in the one complete specimen of *E. leganihanne*, ANSP 21343, width extrapolated from right side preservation, Downs *et al.* 2023).

The dermatocranial ornament of *E. wangsjo* comprises coarse anastomosing ridges that are broken into isolated and conjoined tubercles in some locations, commonly close to the margins of bones (e.g., caudal end of postparietal of NHMD 141833, Fig. 2). The ornament is especially similar to that of *E. leganihanne* ('anastomosing ridges [...] broken into a coarse patten of conjoined tubercles,' Downs *et al.* 2023, p. 5) although, in that species, the tubercles are most concentrated along the dorsal midline of the skull roof. The ornament of *E. wangsjo* is also similar to that of *E. bourdoni*, though coarser (but *E. wangsjo* is also in a different, larger, size category) and with patches of tubercles that are not commonly observed in that species ('finely anastomosing ridges without isolated tubercles,' in *E. bourdoni*, Downs *et al.* 2021, p. 3). It is an ornament that is decidedly different from the pitted ornament observed in several highly nested species of Tristichopteridae (e.g., *Hyneria lindae*, Daeschler & Downs 2018, and *Langlieria radiatus*, Daeschler *et al.* 2019) and additionally in a large-bodied, undescribed tristichopterid from the Britta Dal Formation of East Greenland (pers. obs. of NHMD 141783, 152851).

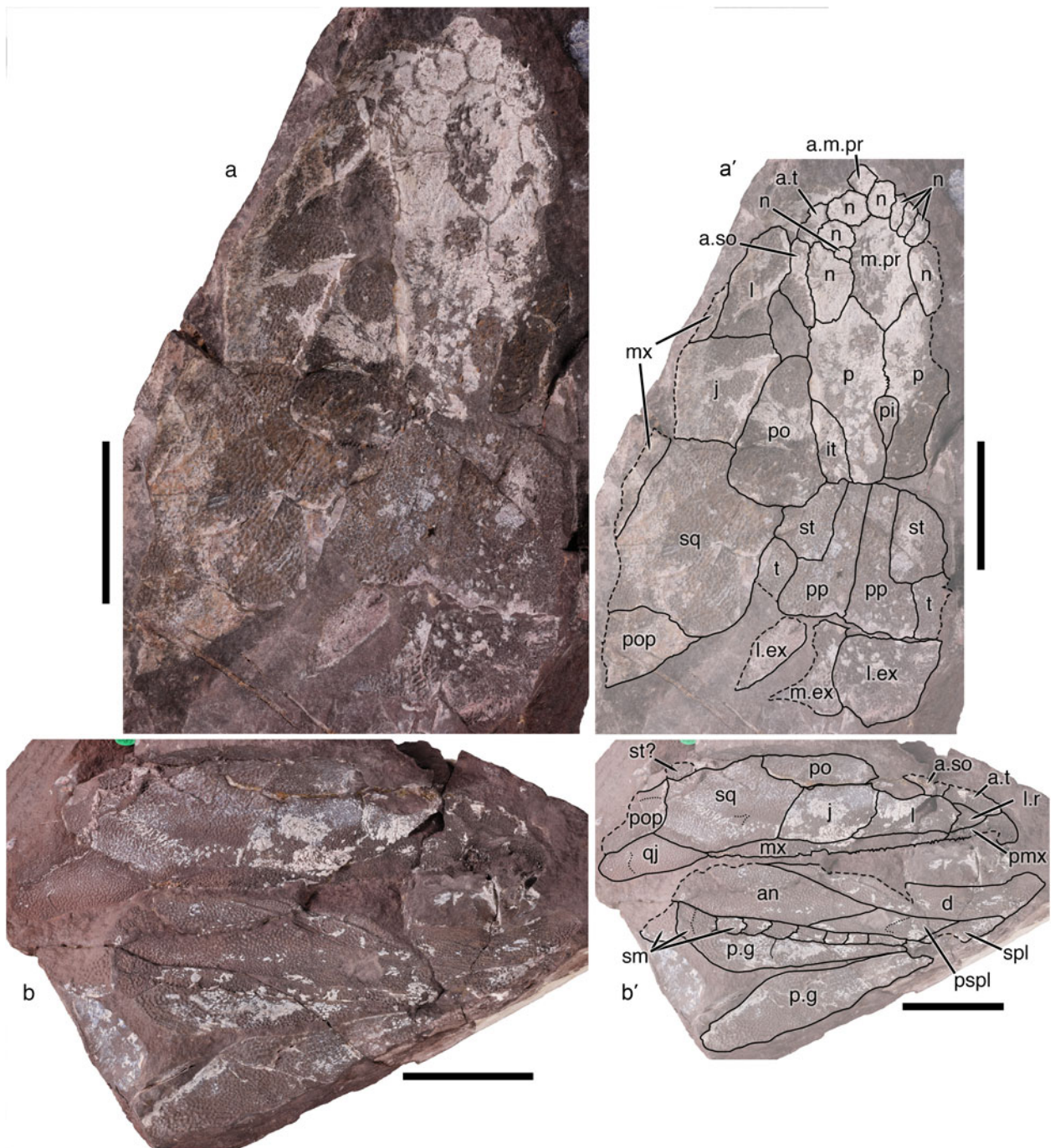


**Figure 2** *Eusthenodon wangsjoii*, NHMD 141833 (holotype), skull primarily in dermal impression: (a) skull roof and right cheek (a, photograph; a', labelled illustration); (b) left cheek, left lower jaw, and operculogular bones (b, photograph; b', labelled illustration). Dotted lines follow pitline grooves; dashed lines follow unfinished bone margins. Abbreviations: a.m.pr = anterior median postrostral; an = angular; a.so = anterior supraorbital; a.t = anterior tectal; d = dentary; it = intertemporal; j = jugal; l = lacrimal; l.ex = lateral extrascapular; l.r = lateral rostral; m.ex = median extrascapular; m.pr = median postrostral; mx = maxilla; n = nasal; p = parietal; p.g = principal gular; pi = pineal bones; pmx = premaxilla; po = postorbital; pop = preopercular; pp = postparietal; pspl = postsplenial; qj = quadratojugal; sm = submandibular; spl = splenial; sq = squamosal; st = supratemporal; t = tabular. Scale bars equal 5 cm.

Pitline grooves are observed on the parietal, postparietal, tabular, squamosal, preopercular, quadratojugal, postsplenial (infradentary 2), second most caudal submandibular and principal gular of *E. wangsjoii*. As in both other species of *Eusthenodon*, the small, hooked (concave caudolaterally) pitline groove of the parietal bone (= frontal pitline of Jarvik 1952) lies entirely rostral to the pineal series of bones. The postparietal bone carries two pitline grooves: the transverse (straight or slightly curved, concave rostral) and, caudal to it, the posterior oblique (often curved, concave caudomedial), both in the caudal half of the bone. A transverse pitline groove of the tabular bone aligns

with the postparietal transverse groove and, in at least NHMD 141691 (Fig. 5a'), is continuous with the postparietal groove across the contact between the bones. This meeting of the transverse pitline grooves of the postparietal and tabular bones is additionally observed in *H. lindae*. The same three pitline grooves, of postparietal and tabular bones, appear in *E. bourdoni* (Downs *et al.* 2021); no specimen informs the condition in *E. leganihanne*. The two pitline grooves of the squamosal that most consistently appear in the *E. wangsjoii* referred materials are in the ventral half of the bone near to midlength. Both are straight or slightly curved and oblique relative to the transverse

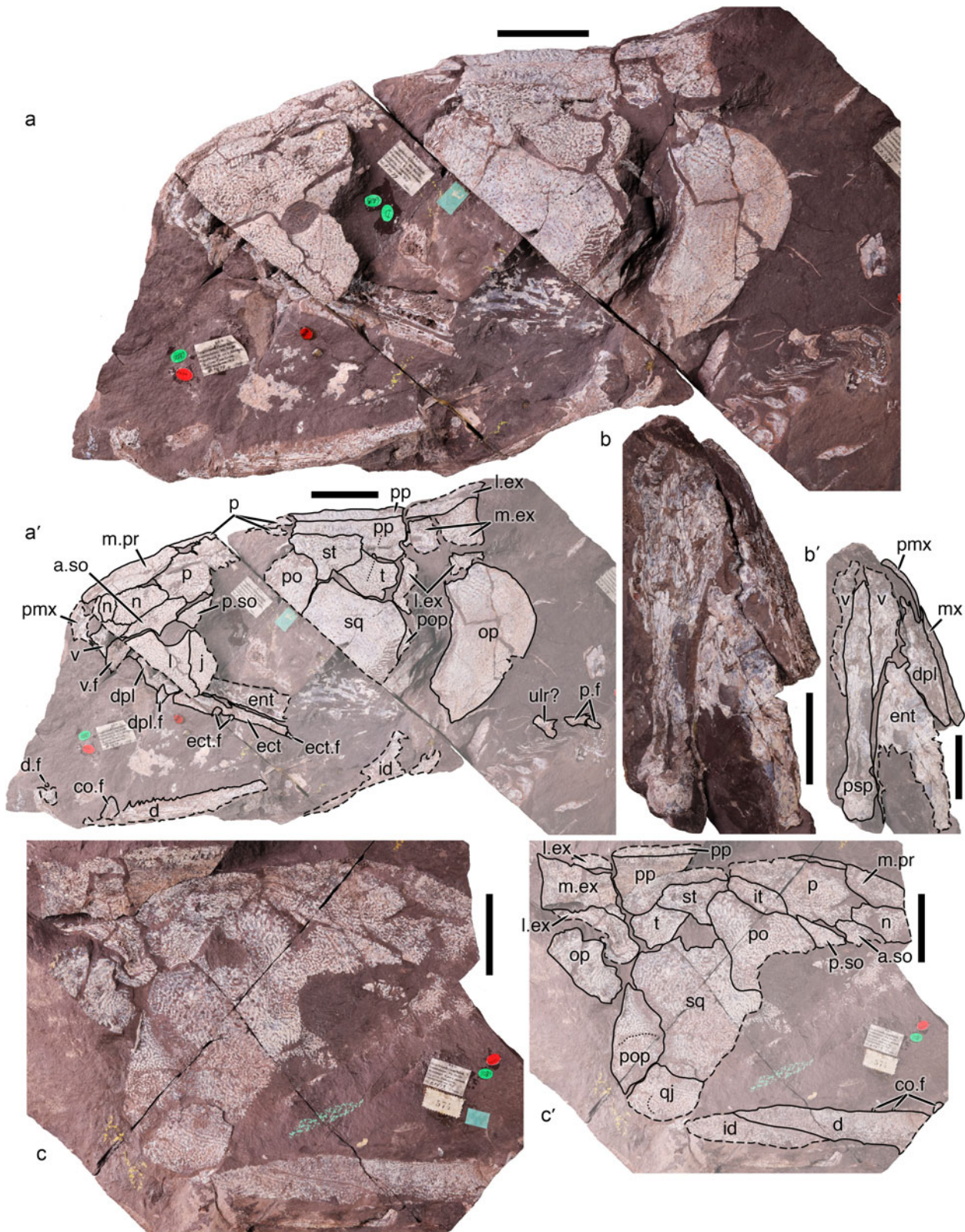


**Figure 3** *Eusthenodon wangsjoii*, NHMD 141653: (a) skull in left lateral view (a, photograph; a', labelled illustration); (b) dermal bones of the palate in palatal view (b, photograph; b', labelled illustration); (c) skull roof, left cheek and left lower jaw primarily in dermal impression, counterpart to (a) (c, photograph; c', labelled illustration). Dotted lines follow pitline grooves; dashed lines follow unfinished bone margins. Abbreviations: a.so = anterior supraorbital; co.f = coronoid fang; d = dentary; d.f = dentary fang; dpl = dermopalatine; dpl.f = dermopalatine fang; ent = entopterygoid; ect = ectopterygoid; ect.f = ectopterygoid fang; id = unidentified infradentary; it = intertemporal; j = jugal; l = lacrimal; l.ex = lateral extrascapular; m.ex = median extrascapular; m.pr = median postrostral; mx = maxilla; n = nasal; op = opercular; p = parietal; p.f = unidentified pectoral fin bones; pmx = premaxilla; po = postorbital; pop = preopercular; pp = postparietal; p.so = posterior supraorbital; psp = parasphenoid; qj = quadratojugal; sq = squamosal; st = supratemporal; t = tabular; ulr? = possible ulnare; v = vomer; v.f = vomerine fang. Scale bars of (a) and (c) equal 5 cm; scale bars of (b) equal 3 cm.

plane; one is dorsal to the other and they are closest to one another at their rostral end and furthest at their caudal end. These pitlines grooves do not meet one another but are otherwise

similar, in position and orientation, to the two limbs of the tightly arched, concave caudoventral pitline groove of the squamosal that is typical for tristichopterids and observed in

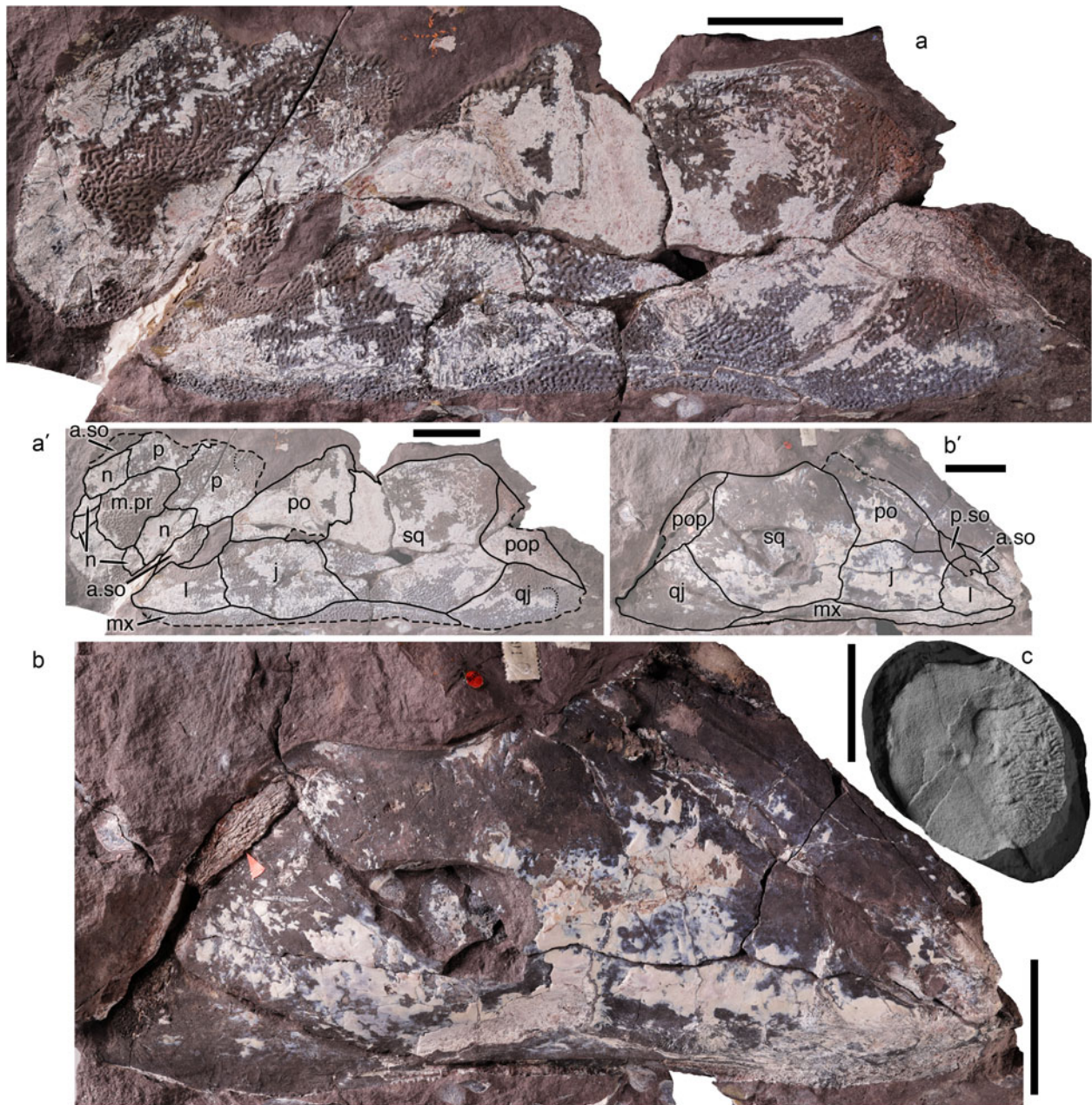


**Figure 4** *Eusthenodon wangsjoii*, NHMD 141689: (a) skull roof and right cheek primarily in dermal impression (a, photograph; a', labelled illustration); (b) right cheek primarily in visceral impression, counterpart to (a) (b, photograph; b', labelled illustration). (c) Scale in dermal view, plaster cast possibly of a latex mould. Dotted lines follow pitline grooves; dashed lines follow unfinished bone margins. The casted rock matrix of (c) was darkened to accentuate margins of the scale. Abbreviations: a.so = anterior supraorbital; j = jugal; l = lacrimal; m.pr = median postrostral; mx = maxilla; n = nasal; p = parietal; po = postorbital; pop = preopercular; p.so = posterior supraorbital; qj = quadratojugal; sq = squamosal. Scale bars of (a) and (c) equal 5 cm; scale bar of (c) equals 2 cm.

the only other species of *Eusthenodon* that preserves the condition (described as 'hook-shaped' in *E. bourdoni*, ANSP 23748, Downs *et al.* 2021, p. 3). A single specimen (NHMD 1201204, Fig. 9a') of *E. wangsjoii* features an oblique (caudodorsal to rostroventral) pitline groove in the caudodorsal corner of the squamosal that aligns with, but is not continuous, the pitline groove of the preopercular. Such a pitline groove is rare among known tristichopterids, but at least one specimen of *Eusthenopteron foordi* (P. 2574, Jarvik 1944) has been described with a long and continuous pitline groove that extends from the caudal half of the preopercular to the rostral half of the squamosal where it hooks ventrally. The more common condition in *E. foordi*, however, is the one typical for tristichopterids, with separate (horizontal) preopercular and (hooklike) squamosal pitline grooves. The pitline groove of the preopercular of *E. wangsjoii* is typical for a tristichopterid in that is flat and

horizontal or slightly curved (concave ventral), near to mid-height of the bone's dermal surface, and may be nearly as wide as the bone itself. The pitline groove of the quadratojugal of the *E. wangsjoii* holotype (NHMD 141833, Fig. 2b') is in the caudal half of the bone, sinuous in shape (concave caudal at its dorsal end and concave rostral at its ventral end), and nearly as tall as the dermal surface of the bone in that position. Other specimens in the type series have a shorter pitline groove, in the same position on the quadratojugal, that is arched (concave rostral) rather than sinuous (e.g., NHMD 141689, Fig. 4a'; 1201204, Fig. 9a') and more consistent with the condition of the groove observed commonly among tristichopterids. The postsplenic carries a single arched (concave mesiodorsal) pitline groove (e.g., NHMD 141693, Fig. 6a') that has not been yet observed in either of the other two species of *Eusthenodon*; at present, specimen availability and preservation may explain its absence in those species.

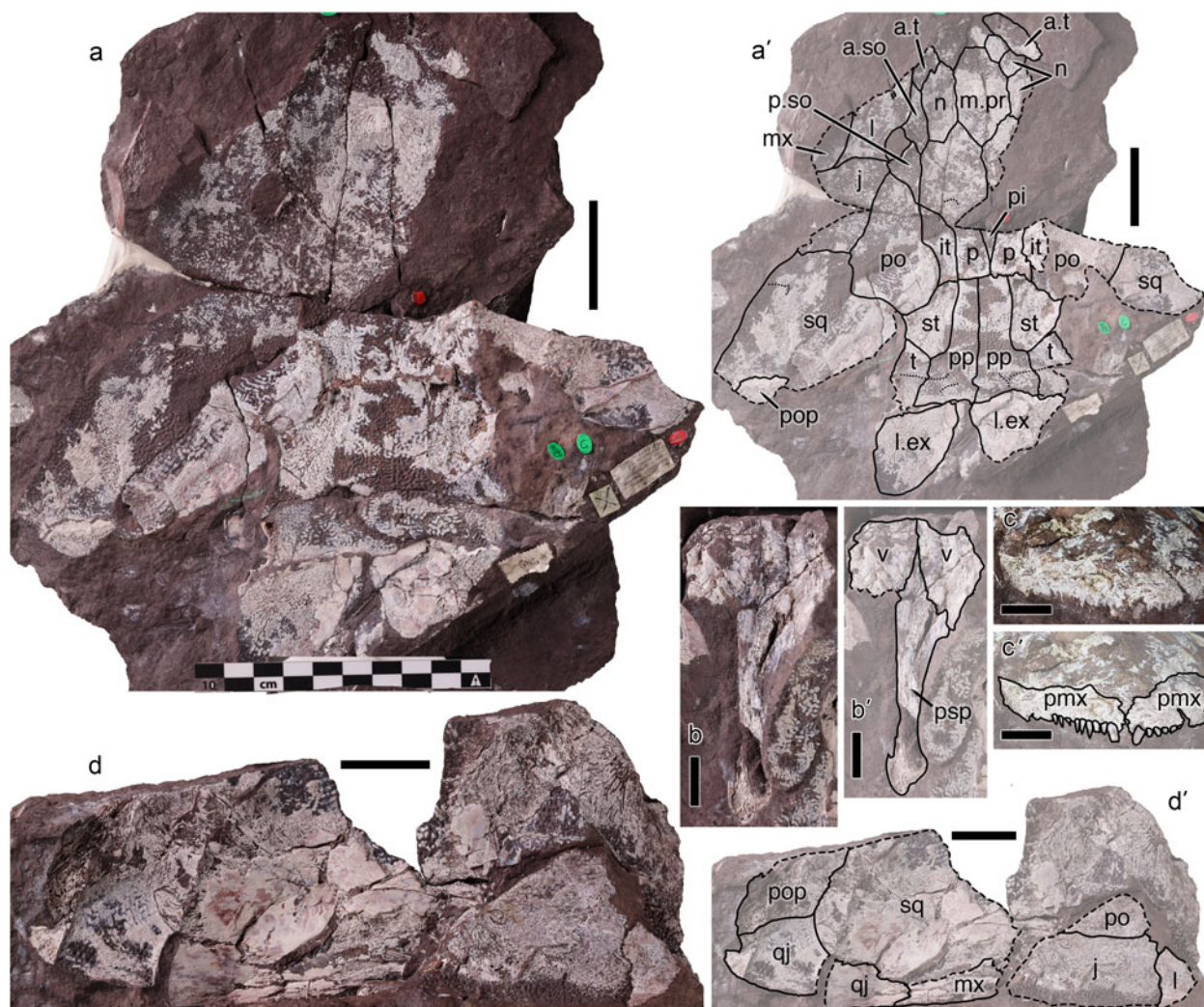


**Figure 5** *Eusthenodon wangsjoii*, NHMD 141691: (a) skull primarily in dermal impression (a, photograph; a', labelled illustration); (b) dermal bones of the palate in visceral view (b, photograph; b', labelled illustration); (c) premaxillae in rostral view (c, photograph; c', labelled illustration); (d) left cheek primarily in visceral view. Dotted lines follow pitline grooves; dashed lines follow unfinished bone margins. Abbreviations: a.so = anterior supraorbital; a.t = anterior tectal; it = intertemporal; j = jugal; l = lacrimal; l.ex = lateral extrascapular; m.pr = median postrostral; mx = maxilla; n = nasal; p = parietal; pi = pineal bones; pmx = premaxilla; po = postorbital; pop = preopercular; pp = postparietal; p.so = posterior supraorbital; psp = parasphenoid; qj = quadratojugal; sq = squamosal; st = supratemporal; t = tabular; v = vomer. Scale bars of (a) equal 5 cm; scale bars of (b) and (c) equal 2 cm; scale bars of (d) equal 3 cm.

The pitline groove of the second most caudal submandibular is a shallow sinuosity (as in NHMD 141833, Fig. 2b') or is curved concave rostral (as in NHMD 141693, Fig. 6a'), close to mid-length, and orthogonal to the bone's long (rostral–caudal) axis. The principal gular has a short, transversely oriented pitline groove that is slightly curved concave caudal, close to the bone's midlength, and near to the lateral margin of the bone (Fig. 6a').

#### 4.2. Parietal shield

Complete and nearly complete parietal shields of *E. wangsjoii*, in a range of sizes, allow for description of the premaxilla, anterior median postrostral and median postrostral, nasal series, anterior and posterior supraorbital, anterior tectal, lateral rostral, parietal, intertemporal and pineal series. Overlapping relationships among many of these bones are difficult to assess given the preservational condition of the specimens; many are divided between part and counterpart blocks, neither of which preserves an entirely dermal or visceral surface. The parietal bone of *E. wangsjoii* (p, Figs 2–5, 8, 12) is long relative to the midline length of the parietal shield and longer in visceral than in dermal view due to the dermal overlap of postrostral and nasal bones onto the parietal (parietal is 60–62% the length of the parietal

shield among the three relevant specimens measured in dermal view: NHMD 141691 [60%], 141833 [holotype, 60%] and 153925 [62%]). In dermal view, the rostral margin of the parietal bone falls within the length of the orbit in *E. wangsjoii*. Among tristichopterids, a parietal that reaches rostral to the orbit is uncommon with *Hyneria lindae* (in visceral view only, Daeschler & Downs 2018, fig. 3) and *Cabonnichthys burnsi* (in at least dermal view, Ahlberg & Johanson 1997, figs 4a, 5a) the only recorded examples. NHMD 1201214, described and referred to cf. *E. wangsjoii* later in the present work, also shows a parietal bone reaching rostral to the orbit in visceral view (the only view available; see section 6.2.1). *Eusthenodon bourdoni* shows a comparable condition to that of *E. wangsjoii*, in that the rostral margin of the parietal is nearly aligned with the rostral margin of the orbit in visceral view and is within the orbit in dermal view (Downs *et al.* 2021, figs 2a, 3a). In *Eusthenodon leganihanne*, the rostral reach of the parietal bone is within the length of the orbit in both dermal and visceral views (Downs *et al.* 2023, figs 2, 7b).

In articulated specimens in dermal view, the rostral margin of the parietal bone appears deeply notched where it accommodates the overlap of the caudally pointed, most caudal element in the nasal series. In the one relevant specimen of *E. bourdoni*

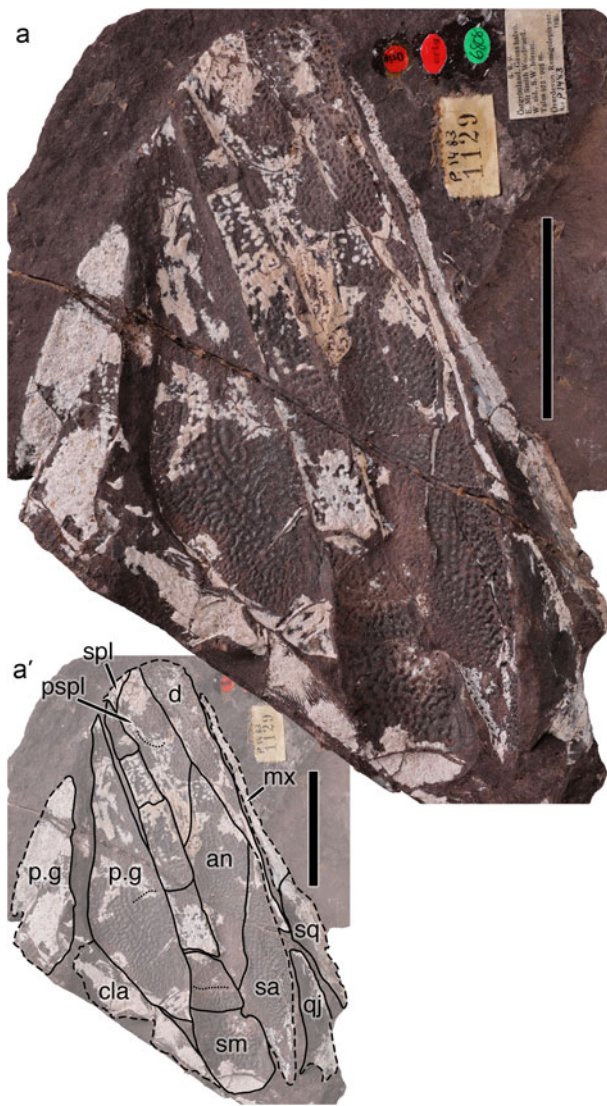


**Figure 6** *Eusthenodon wangsjoi*, NHMD 141693: (a) partial right cheek, right lower jaw and operculogular bones primarily in dermal impression (a, photograph; a', labelled illustration). Dotted lines follow pitline grooves; dashed lines follow unfinished bone margins. Abbreviations: an = angular; cla = clavicle; d = dentary; mx = maxilla; p.g = principal gular; pspl = postsplenial; qj = quadratojugal; sa = surangular; sm = submandibular; spl = splenial; sq = squamosal. Scale bars equal 5 cm.

(ANSP 25037, Downs *et al.* 2021, fig. 3a), the ornamented surface of the right parietal shows a shallow notch where the caudal nasal bone overlaps, but the left parietal is without such a notch. No specimen of *E. leganihanne* informs this condition. In the largest specimens of *E. wangsjoi*, the parietal is relatively narrow (width/length ratio between 0.34 and 0.40 in the three largest specimens by parietal length, all of which are preserved dermally: NHMD 141653 [0.40], 141691 [0.37], 153925 [0.39, right; 0.34, left]). Relatively wider parietal bones are observed in smaller specimens, such that the full range of width/length ratios for the parietal bone in *E. wangsjoi* is 0.35 to 0.53 when all six relevant specimens are considered (including additionally NHMD 141833 [holotype, 0.44, preserved dermally], 1201203 [0.52, right, dermal; 0.52, left, visceral] and 1201222 [0.53, dermal]). In *E. leganihanne*, the width/length ratio of the parietal bone is 0.45 in a large individual (by parietal length, ANSP 21342, preserved dermally) and 0.34 in a smaller one (ANSP 21343, holotype, preserved viscerally). Two specimens of *E. bourdoni* (ANSP 25038, 23748) show the opposite trend, with the smaller specimen (by parietal length) having the relatively wider parietal

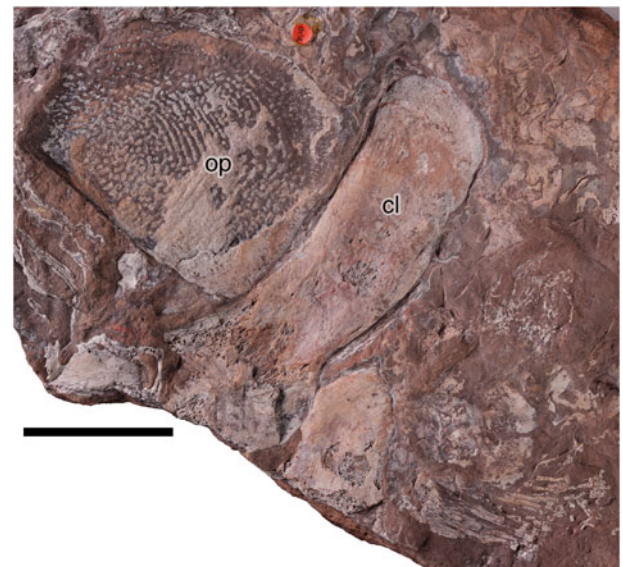


**Figure 7** *Eusthenodon wangsjoi*, NHMD 141694, right opercular primarily in dermal impression, and right cleithrum and bones of the right pectoral fin in visceral view. Abbreviations: cl = cleithrum; op = opercular. Scale bar equals 5 cm.

bones, at least in its dermal, articulated preservation that undermeasures parietal length but not width (ANSP 25037, width/length ratios of 0.48, left parietal, and 0.51, right; compared to 0.43, left visceral, and 0.40, right visceral, in ANSP 23748).

The premaxilla of *E. wangsjoi* (pmx, Figs 2, 3, 5, 8) is deepest at its mesial end but is not well preserved in any of the available specimens in the type series, so more detailed anatomical description of the bone's shape is impossible. The premaxillary tooth row is best preserved in NHMD 141691 (Fig. 5c'). It is observed to include a single, enlarged tusk at its mesial end; this tusk is in line with the bone's marginal teeth and the marginal teeth do not increase in size with proximity to the tusk (palatal dental morphotype C of Borgen & Nakrem 2016). A single, enlarged tusk is expected in a highly nested tristichopterid, though recent phylogenetic analyses (including those of Downs & Daeschler 2022 and Downs *et al.* 2023) have incorrectly presented *E. wangsjoi* as an outlier, with premaxillary marginal teeth that increase in size with proximity to the mesial end of the bone but without a single enlarged tusk. Between the two other species of *Eusthenodon*, only *E. leganihanne* has material to inform the condition of the premaxillary tooth row, and that species also has a single, enlarged premaxillary tusk (Downs *et al.* 2023).

The median postrostral of *E. wangsjoi* (m.pr, Figs 2–5, 8, 12) is an elongate (width/length ratio of 0.54 in the holotype, NHMD 141833, in dermal view), multi-sided bone that substantially overlaps the parietal bones. It is bordered laterally by the nasal series of the bones, the most caudal of which separates the median postrostral from the anterior supraorbital bone. The most caudal nasal bone is consistently the largest bone in a series that otherwise varies greatly in the sizes of the elements, the number of elements, and the symmetry left to right. Among the specimens in the type series, between three and five nasals are observed on a single side and the number of bones need not be equal on left and right sides of a single specimen; the holotype (NHMD 141833) has five nasals on the left and four on the right, with one on the right small enough to allow the nasal bones bordering it to contact one another. The caudal nasal bone narrows to a blunt caudal point that fits into the notched rostral margin of the parietal. Left and right nasal series meet at the midline rostral to the median postrostral. Rostral to the

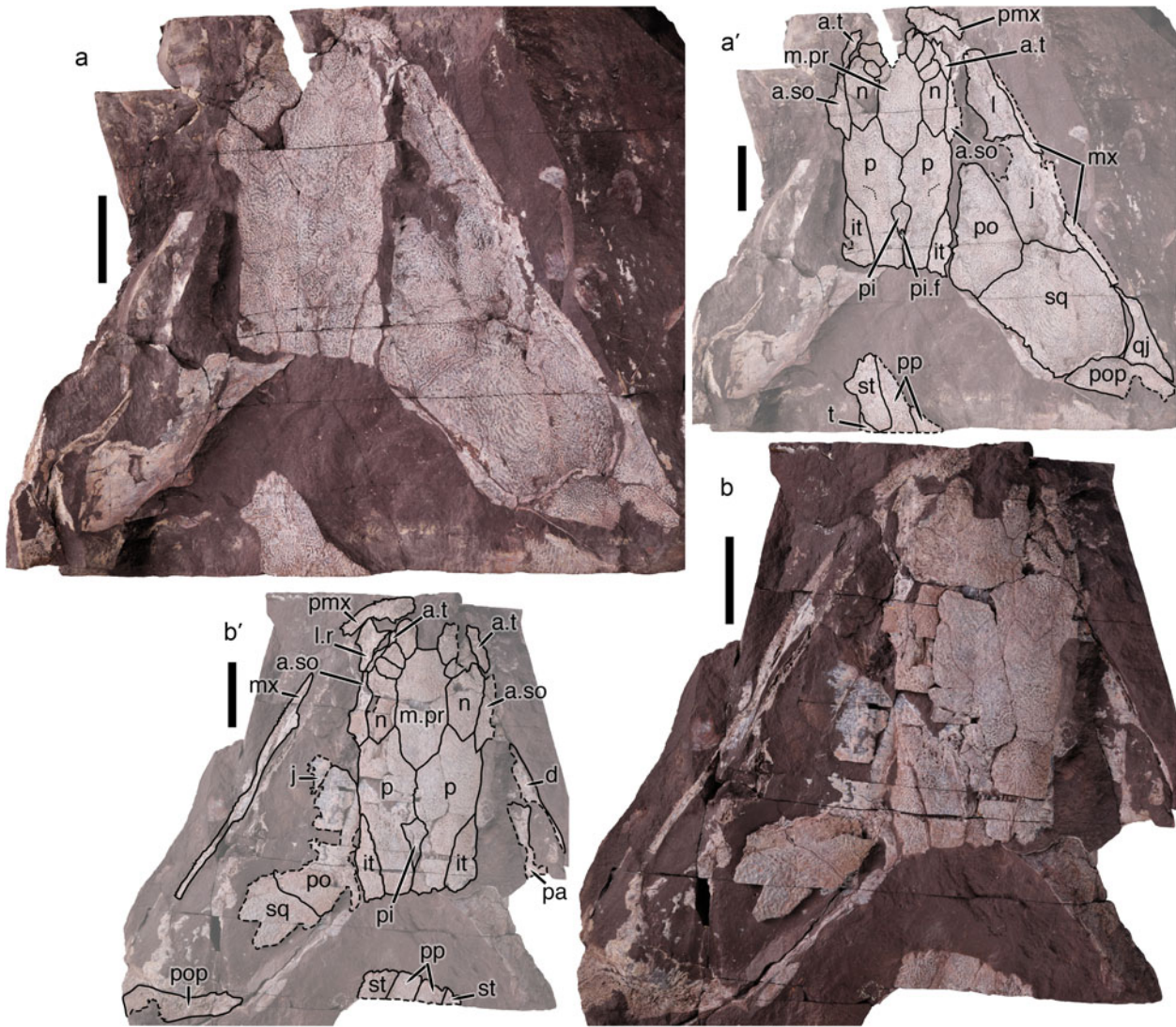


**Figure 8** *Eusthenodon wangsjoii*, NHMD 153925: (a) skull and left cheek primarily in dermal impression (a, photograph; a', labelled illustration); (b) skull roof and left cheek in dermal view, counterpart to (a) (b, photograph; b', labelled illustration). Dotted lines follow pitline grooves; dashed lines follow unfinished bone margins. Abbreviations: a.so = anterior supraorbital; a.t = anterior tectal; d = dentary; it = intertemporal; j = jugal; l = lacrimal; l.r = lateral rostral; m.pr = median postrostral; mx = maxilla; n = nasal; p = parietal; pa = prearticular; pi = pineal bones; pi.f = pineal foramen; pmx = premaxilla; po = postorbital; pop = preopercular; pp = postparietal; qj = quadratojugal; sq = squamosal; st = supratemporal; t = tabular. Scale bars equal 5 cm.

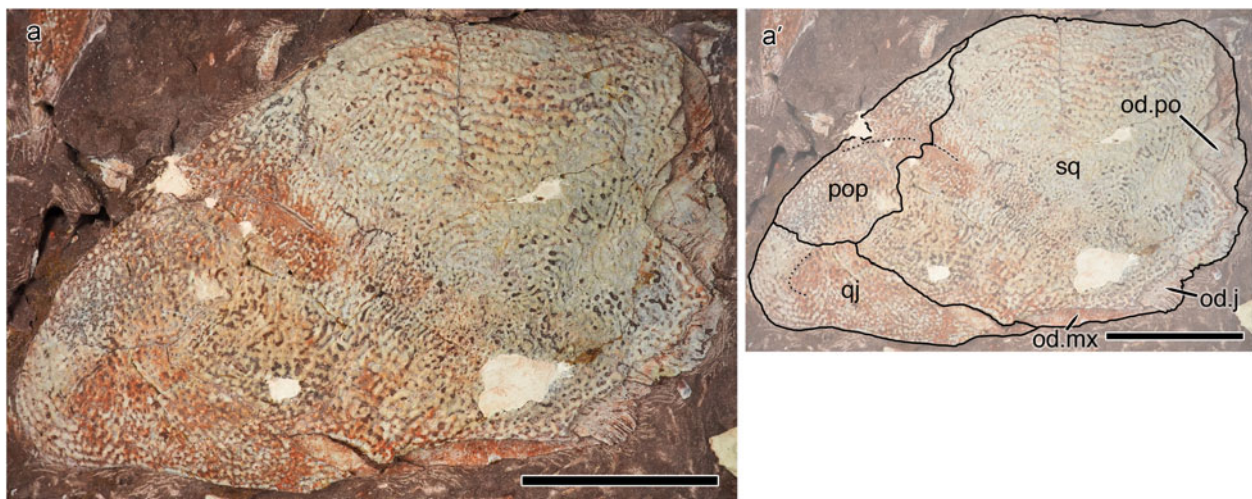


**Figure 9** *Eusthenodon wangsjoii*, NHMD 1201204: (a) partial right cheek in dermal view (a, photograph; a', labelled illustration). Dotted lines follow pitline grooves. Abbreviations: od.j = area overlapped by the jugal; od.mx = area overlapped by the maxilla; od.po = area overlapped by the postorbital; pop = preopercular; qj = quadratojugal; sq = squamosal. Scale bars equal 5 cm.

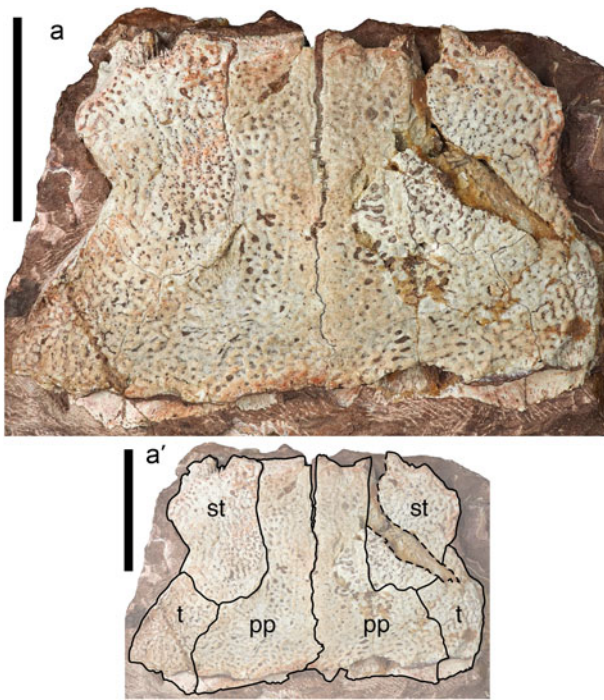


**Figure 10** *Eusthenodon wangsjoii*, NHMD 1201205: (a) postparietal shield in dermal view (a, photograph; a', labelled illustration). Dashed lines follow unfinished bone margins. Abbreviations: pp = postparietal; st = supratemporal; t = tabular. Scale bars equal 5 cm.

nasals, on the midline, is a wide diamond-shaped anterior median postrostral (a.m.pr; Fig. 2; = anterior postrostral of Jarvik 1952). Detailed description of the rostral end of the parietal shield has not been possible in the two other species of *Eusthenodon*. Bone margins are impossible to discern in the one specimen of *E. leganihanne* that preserves the rostral parietal shield (ANSP 21342) and does so in exclusively dermal view. In both parietal shield specimens of *E. bourdoni* (ANSP 23748, 25037), the margins of the median postrostral and the most caudal nasal bone in each series, but no more rostral elements, may be discerned due to incomplete preservation.

The pineal series in *E. wangsjoii* (pi, Figs 2, 5, 8, 12) forms a teardrop-shaped (pointed end caudal) cluster of bones at the caudal end of the parietal shield's midline, in dermal view. This is the expected condition for a highly nested tristichopterid and differs from the circular to ovoid, rostrally located series in *Eusthenopteron foordi* (Jarvik 1944). In some of the *E. wangsjoii*

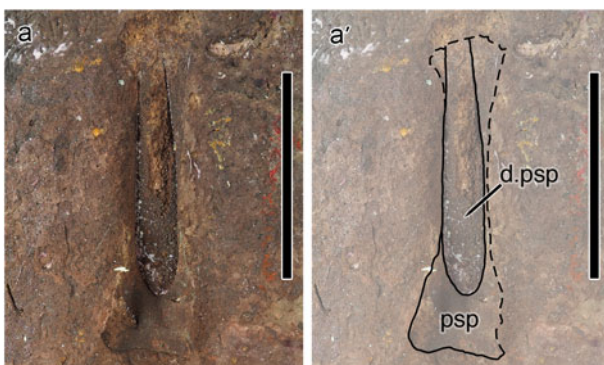


**Figure 11** *Eusthenodon wangsjoii*, NHMD 1201211: (a) parasphenoid in dermal impression (a, photograph; a', labelled illustration). Dashed lines follow unfinished bone margins. Abbreviations: d.psp = denticulated surface of parasphenoid; psp = parasphenoid. Scale bars equal 5 cm.

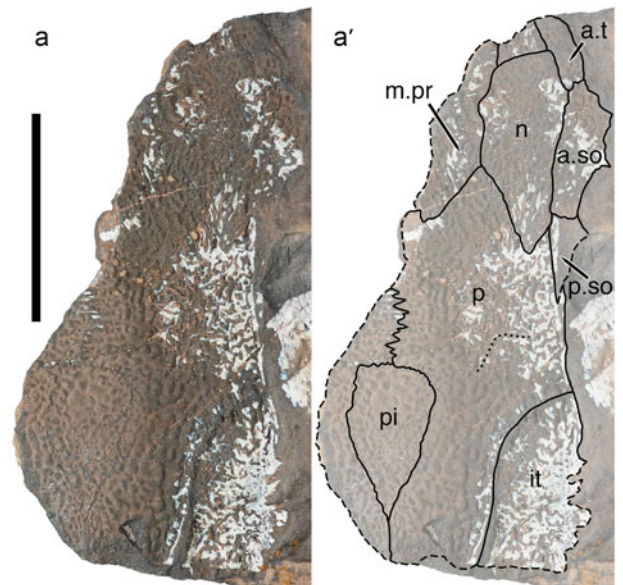


**Figure 12** *Eusthenodon wangsjoii*, NHMD 1201222: (a) partial parietal shield primarily in dermal impression (a, photograph; a', labelled illustration). Dashed lines follow unfinished bone margins. Abbreviations: a.so = anterior supraorbital; a.t = anterior tectal; it = intertemporal; m.pr = median postrostral; n = nasal; p = parietal; pi = pineal bones; p.so = posterior supraorbital. Scale bar equals 5 cm.

specimens preserved in dermal view (e.g., NHMD 153925, Fig. 8a'), the rostral, wider end of the pineal series is also pointed. In most specimens, the pineal bones are entirely caudal to the rostral end of the intertemporals, in dermal view. However, at least one specimen (NHMD 1201222, Fig. 12), preserved in dermal impression, has a pineal series that extends rostral to the intertemporal. In at least one specimen (NHMD 153925, Fig. 8a'), the pineal bones surround a circular pineal foramen that is located in the caudal half of the pineal area. The pineal series of bones in *E. bourdoni*, in both dermal (ANSP 25037; Downs *et al.* 2021, fig. 3a) and visceral (ANSP 23748; Downs *et al.* 2021, fig. 2a) views, is teardrop-shaped, with a caudally positioned foramen, and is entirely caudal to the rostral reach of the intertemporals. The pineal series of *E. leganihanne* is poorly represented by the referred materials but the parietal shield of the holotype (ANSP 21343; Downs *et al.* 2023, fig. 2) does show that the collective of bones tapers to a caudal point and is entirely caudal to the rostral reach of the intertemporals.

The intertemporal bone of *E. wangsjoii* (it, Figs 2, 3, 5, 8, 12), like the one in *E. bourdoni* (Downs *et al.* 2021) and in *E. leganihanne* (Downs *et al.* 2023), is a long, narrow bone with nearly parallel lateral and medial margins for much of its length and a rostral end that tapers to a lateral point. Because of dermal overlap of intertemporal onto the parietal, in articulated specimens of all three species of *Eusthenodon*, the full length of the intertemporal is only visible in dermal view. Length measurements for the intertemporal are undermeasured, then, in articulated specimens in visceral view. Because width measurements are nearly equal in both views, the width/length ratio of the bone, in articulated specimens, is overmeasured in visceral view. Only two of the *E. wangsjoii* specimens considered here (NHMD 141653, 153925), both articulated parietal shields in dermal view, inform the intertemporal/parietal length ratio (0.48, NHMD 141653; and 0.56, NHMD 153925) and the width/length ratio of the intertemporal (0.30, NHMD 141653; and 0.32, NHMD 153925). These values compare favourably with those of *E. leganihanne* (intemporal/parietal length ratio of 0.55, ANSP 21343 [holotype]; intertemporal width/length ratio of 0.30, ANSP 21342) and *E. bourdoni* (intemporal/parietal

length ratio of 0.52, ANSP 25037; intertemporal width/length ratio of 0.31 [left] and 0.33 [right], ANSP 25037). A long and narrow intertemporal is common among highly nested tristichopterids, though at least *Langlieria smalingi* (Downs & Daeschler 2022, fig. 3) exhibits a short and wide intertemporal that is restricted to the caudolateral corner of the parietal shield.

The anterior supraorbital bone of *E. wangsjo* (a.so, Figs 2–5, 8, 12) lies lateral to the most caudal, and largest, nasal bone and forms the dorsorostral portion of the orbital margin. The anterior supraorbital makes a longer contribution to the orbital margin than does the posterior supraorbital and the length of the anterior supraorbital that extends rostral to its orbital margin is longer than the bone's contribution to the orbit. Though only the holotype (NHMD 141833) shows all three bones, rostral to the anterior supraorbital bone is an elongate anterior tectal bone (a.t, Figs 2, 5, 8, 12) and ventral to it, a lateral rostral bone (l.r, Fig. 2). The posterior supraorbital bone in *E. wangsjo* (p.so, Figs 3–5, 12) forms the dorsocaudal corner of the orbital margin and has an elongate, pointed, caudal process. The caudal process is considerably longer than the bone's orbital margin and is therefore comparable in its dimensions to that of most other highly nested tristichopterids, though not *Edeonopteron keithcrooki* (Young *et al.* 2019) nor, notably, *E. leganihanne* (Downs *et al.* 2023). The posterior supraorbital of *E. wangsjo* is similar to that of *E. leganihanne* in that it contacts the lacrimal ventrally so only three bones (anterior supraorbital, posterior supraorbital and lacrimal) contribute to the orbital margin. *Eusthenodon bourdoni* differs by having a jugal bone that contributes substantially to the orbital margin, a feature that helps to diagnose the species (Downs *et al.* 2021, fig. 2). The posterior supraorbital bone of *Eusthenodon*, like the intertemporal, also overlaps the parietal and postorbital so the proximity of posterior supraorbital and intertemporal bones is undermeasured in visceral view. In *E. bourdoni*, for example, the bones have been interpreted to contact one another in dermal view but not visceral view, allowing supraorbital–intertemporal contact dermally and parietal–postorbital bones viscerally (Downs *et al.* 2021). No specimen in the *E. wangsjo* type series convincingly shows contact between the posterior supraorbital and the intertemporal. In the holotype (NHMD 141833), the right intertemporal is visible in dermal impression, but the right posterior supraorbital is missing. The surrounding bones are present and in place and dermal contact between parietal and postorbital is observed. This necessitates some degree of separation between posterior supraorbital and intertemporal. Only one specimen in the type series (NHMD 141691, Fig. 5a) shows both a complete intertemporal and a posterior supraorbital bone in place on a single side. In NHMD 141691, preserved dermally, interpretation of the relationship between these bones is challenged by the dermal surface of the skull only being available in impression; in addition, cracks through the rock disrupt the margins of the intertemporal. In this specimen, the posterior supraorbital and intertemporal do appear in close proximity but contact cannot be confirmed. In Jarvik's (1952, text-figs. 23b, 25a) illustrations of this specimen (then designated P. 1478), the two bones are separated, but careful study of the specimen's part and counterpart blocks does not offer convincing support for this interpretation. It is, however, this interpretation of this specimen that appears to inform Jarvik's (1952, text-fig. 26) skull reconstruction and his description of the posterior supraorbital ('the bone ends a little in front of the [intertemporal];' Jarvik 1952, p. 62). In the relatively complete parietal shield of NHMD 153925 (Fig. 8), preserved dermally, both posterior supraorbital bones are missing, but the great distance between anterior supraorbital and intertemporal (4.7 cm in a skull with a 6.0 cm long intertemporal) supports a considerable separation between posterior supraorbital and

intertemporal. A lack of contact between the two bones is the more common condition among highly nested tristichopterid species, although contact is observed in *Cabonnichthys burnsi* (Ahlberg & Johanson 1997) and dermal contact has been inferred in *E. bourdoni* (Downs *et al.* 2021).

#### 4.3. Postparietal shield

Among the relevant specimens (NHMD 141833, 141653, 141691, 153925, 1201205), all of the available bones of the *E. wangsjo* postparietal shield (postparietal, supratemporal and tabular) belong to articulated specimens preserved in dermal view or dermal impression. As a result, these do not allow description of any potential features of the visceral surface, including the median ridge and ventral lamina of the supratemporal and tabular that are commonly observed in tristichopterids, including in both other species of *Eusthenodon* (Downs *et al.* 2021, 2023). The postparietal bone of *E. wangsjo* (pp, Figs 2, 3, 5, 8, 10) has a caudal margin width that is more than double its rostral margin width (caudal width/rostral width ratio of 2.21 in the holotype, NHMD 141833, and between 2.21 and 2.71 among the three relevant specimens, including, additionally, NHMD 141691 [2.71] and 1201205 [2.70]). The ornamented surface of the postparietal does not widen gradually, instead changing width in a stepped fashion at a position in line with the supratemporal/tabular contact. The added width of the postparietal in its caudal half overlaps the tabular bone such that the maximum width of the postparietal bone is only observed in dermal view of articulated specimens. In *E. wangsjo*, the postparietal's caudal width/rostral width ratio has a range of values that approximates the values measured in *E. bourdoni* (~2.8 in ANSP 25037, though caudal margin width is estimated due to the incomplete nature of the specimen; Downs *et al.* 2021) and in *E. leganihanne* (~2.6 in ANSP 21343; Downs *et al.* 2023). The caudal margins of the dermal surface of the postparietal and tabular bones carry a long, depressed, unornamented zone to accommodate the overlap of the median and lateral extrascapular bones. These extrascapular overlap zones are best observed in NHMD 1201205 (Fig. 10) where they appear to be continuous along the entirety of the postparietal shield's caudal margin with a narrow gap across the midline. These overlap zones also appear in *E. bourdoni* (Downs *et al.* 2021); the condition is presently impossible to address in *E. leganihanne* (Downs *et al.* 2023).

The tabular (t, Figs 2, 3, 5, 8, 10), broadly overlapped by the postparietal, has a narrow ornamented zone that carries the bone's pitline groove. The tabular forms much of the deeply notched portion of the postparietal shield's lateral margin, a feature that has been labelled a spiracular notch in *Langlieria socqueti* ('Tristichopteridae gen. et sp. indet.' of Clément 2002, p. 582; Clément *et al.* 2009) and which appears in both *E. bourdoni* (Downs *et al.* 2021) and *E. leganihanne* (Downs *et al.* 2023).

The supratemporal of *E. wangsjo* (st, Figs 2, 3, 5, 8, 10) is consistently longer than the tabular bone. It flares rostrally to form a short extension that reaches beyond the rostral margin of the postparietal bone. This extension of the supratemporal then differs in shape from the pronounced rostralateral horn-like process (concave rostromedial, convex caudolateral) of the supratemporal's ornamented surface in *E. bourdoni* (Downs *et al.* 2021), *E. leganihanne* (Downs *et al.* 2023) and *Hynieria lindae* (Daeschler & Downs 2018). Some degree of rostral extension of the supratemporal has additionally been reported in *Eusthenopteron foordi* (Jarvik 1944), *Eusthenopteron säve-söderberghi* (Jarvik 1944; Clément 2002), and in *Tristichopterus alatus* (Snitting 2008). In *E. wangsjo*, and similar to the condition in *E. bourdoni* (Downs *et al.* 2021), there is a depressed, unornamented area in the rostralateral corner of the supratemporal's dermal surface to accommodate overlap of the postorbital

bone (Fig. 10); the condition in *E. leganihanne* is impossible to address given the available material (Downs *et al.* 2023). The supratemporal of *E. wangsjoii* also flares laterally to form the rostral margin of the postparietal shield's lateral notch.

#### 4.4. Cheek

Complete, articulated cheek specimens of *E. wangsjoii* allow for description of the maxilla, lacrimal, jugal, postorbital, squamosal, preopercular and quadratojugal bones. Several articulated specimens (NHMD 141653, 141691) preserve the entirety of the orbital margin, showing it to be lenticular in shape and longer than it is tall (Figs 3, 5), similar to the orbital shape in both *Eusthenodon bourdoni* (Downs *et al.* 2021) and *Eusthenodon leganihanne* (Downs *et al.* 2023), and additionally in several other highly nested tristichopterids for which the orbital margin is complete enough to determine shape (including *Cabonnichthys burnsi*, Ahlberg & Johanson 1997; and *Mandageria fairfaxi*, Johanson & Ahlberg 1997). Not all highly nested tristichopterids have a lenticular orbital margin, however; that of *Hynieria lindae* (Daeschler & Downs 2018) is distinctly circular. The lacrimal of *E. wangsjoii* forms approximately half of the orbital margin; the anterior and posterior supraorbitals are the only other bones to contribute to the margin; contact between lacrimal and posterior supraorbital separates jugal and postorbital from the orbital margin. Several other tristichopterids are observed with only these three bones in the orbital margin; these include *E. leganihanne* (Downs *et al.* 2023) and additionally *Platycephalichthys bischoffi* (Vorobyeva 1962), *M. fairfaxi* (Johanson & Ahlberg 1997) and *Edenopteron keithcrooki* (Young *et al.* 2013, 2019). The jugal forms a significant portion of the orbital margin in *E. bourdoni*, an anatomical feature that, according to the diagnosis of the species, helps to distinguish it from the *Eusthenodon* type species. A jugal in the orbital margin is otherwise the expected condition for a tristichopterid as the condition appears in all other species with a complete orbital margin. No highly derived tristichopterid species has five bones (with postorbital the fifth) contributing to the orbit, but this condition is common among more basal tristichopterids; the postorbital joins the jugal in the orbital margin of *Tristichopterus alatus* (Snitting 2008), *Heddeleichthys dalgleisiensis* (Snitting 2009), and both species of *Eusthenopteron* for which a complete orbit is preserved (*Eusthenopteron foordi*, Jarvik 1944; and *Eusthenopteron wenjukowi*, Vorobyeva 1977 [= *Jarvikina wenjukowi* of that work]).

The maxilla of *E. wangsjoii* (mx, Figs 2–6, 8) is subequal in height between the bone's two tallest positions, at the lacrimal–jugal contact and at the jugal–squamosal contact. This is the maxilla shape found in all other highly nested members of the clade, but it is contrary to Jarvik's (1952) reporting that the maximum height of the *E. wangsjoii* maxilla is in the rostral half of the bone. This shape interpretation was later reinforced by Jarvik (1985; see section 6.2.4) and all others citing his descriptions, including the cladistic analyses of Olive *et al.* (2020), Downs & Daeschler (2022) and Downs *et al.* (2023). My observations of Jarvik's (1952, 1985) study specimens support the understanding that no known tristichopterid maxilla is tallest in the rostral half. A maximum maxillary height in the caudal half is found only in basal tristichopterids that lack a pronounced rostradorsal process between lacrimal and jugal (the species of *Tristichopterus*, Snitting 2008; *Eusthenopteron*, Jarvik 1944, Vorobyeva 1977; *Platycephalichthys*, Vorobyeva 1962; and *Heddeleichthys*, Snitting 2009).

Among the *E. wangsjoii* type series of specimens, an articulated, partial cheek specimen (NHMD 1201204, P. 1474 of Jarvik 1952; Fig. 9) lacks the maxilla bone but the ventral margin of the squamosal shows a depressed, unornamented zone to accommodate maxilla overlap (overlap zone labelled 'od1Mx, area of squamosal overlapped by maxillary' by Jarvik 1952,

fig. 28). The opposite relationship (squamosal overlap onto the maxilla) is the more common condition among tristichopterids and is present in both other species of *Eusthenodon*, *E. bourdoni* (see ANSP 23748, Downs *et al.* 2021, fig. 2b) and *E. leganihanne* (see ANSP 21649, Downs *et al.* 2023, fig. 8b). Recent phylogenetic analyses (including Olive *et al.* 2020; Downs & Daeschler 2022; Downs *et al.* 2023) have scored the condition in *E. wangsjoii* according to NHMD 1201206 and Jarvik's (1985) description of it. In the phylogenetic analysis associated with this work, the condition in *E. wangsjoii* is scored according to the condition in NHMD 1201204, the only specimen in consideration that informs the squamosal–maxilla relationship. Maxilla overlap onto the squamosal is otherwise observed in only three known tristichopterid species, among which are two highly nested members of the clade; these three are *Eusthenopteron foordi* (Jarvik 1944), *Hynieria lindae* (Daeschler & Downs 2018) and *Langhleria smalingi* (Downs & Daeschler 2022). In *E. wangsjoii*, the maxilla also overlaps the quadratojugal.

The lacrimal of *E. wangsjoii* (l, Figs 2–5, 8) is a long bone that contacts anterior and posterior supraorbital, jugal, maxilla and lateral rostral bones. A pointed dorsal process at the caudal end of the lacrimal forms the posterior supraorbital contact point that isolates jugal and postorbital from the orbital margin. The rostral end of the lacrimal extends well beyond the orbit (56% of total length is rostral to the bone's orbital margin in the one relevant specimen, NHMD 153925; Fig. 8). This condition, half or more of the lacrimal extending rostral to the orbit, is similar to that of *E. bourdoni* (54% of lacrimal rostral to orbit in ANSP 23748 [holotype]; 48% in ANSP 25037; Downs *et al.* 2021) in addition to those of *H. lindae* (Daeschler & Downs 2018), *Tinirau clackae* (Swartz 2012) and *M. fairfaxi* (Johanson & Ahlberg 1997). In *E. leganihanne* (Downs *et al.* 2023), the lacrimal is differently shaped in that the rostral margin of the bone is angled steeply ventral from the orbital margin such that only 40% of total lacrimal length (same measurement in both relevant specimens: ANSP 21343, 21651) is rostral to the lacrimal's orbital margin.

The jugal of *E. wangsjoii* (j, Figs 2–5, 8) is rectangular and longer than tall. The available material supports its overlap onto the maxilla but the nature of its contacts with other surrounding bones is impossible to determine from the type specimens. The length of the jugal places the point of contact among jugal, postorbital, and squamosal in the caudal half of the postorbital's ventral margin in dermal view (at 58–84% of total rostral-to-caudal length of the margin among the four relevant specimens: NHMD 141833 [holotype, 58%], 141689 [73%], 141691 [71%], 153925 [84%]). The condition in the one relevant specimen of *E. bourdoni* is close to the upper end of the variation observed in the type species (at 78% of total rostral-to-caudal length of the postorbital ventral margin in ANSP 23748), suggesting a long jugal in that species. No specimen of *E. leganihanne* preserves enough of the jugal and postorbital to measure the position of this three-bone point of contact, but partial cheek specimens that are referred to the species (ANSP 21342, 21651, 21652), all in dermal view or dermal impression, reveal a long jugal with a jugal–squamosal–postorbital contact point closer to the caudal end of the postorbital's ventral margin than to its midpoint. A jugal long enough to put the jugal–squamosal–postorbital contact point close to the caudal end of the postorbital is common among highly nested tristichopterids (observed additionally in *M. fairfaxi*, Johanson & Ahlberg 1997; *C. burnsi*, Ahlberg & Johanson 1997; *H. lindae*, Daeschler & Downs 2018; and *E. keithcrooki*, Young *et al.* 2019).

The postorbital (po, Figs 2–5, 8) of *E. wangsjoii*, narrow at its rostral end, increases gradually in height rostral to caudal and, at its caudal end, shortens abruptly to a dorsocaudal pointed

terminus. The caudal end of the postorbital fits into the dorsal concavity in the ornamented surface of the squamosal's rostral margin, and the caudal point of the postorbital lies at the squamosal's dorsorostral corner. The postorbital overlaps the squamosal and supratemporal bones and is overlapped by the posterior supraorbital; the *E. wangsjoii* specimens considered for this description do not explicitly reveal the nature of the relationship between postorbital and its other bordering bones: jugal, parietal and intertemporal.

The squamosal (sq, Figs 2–6, 8, 9) of *E. wangsjoii* is the tallest bone of the cheek, reaching from its contact with the maxilla to the dorsal edge of the cheek. The rostral margin of the squamosal's ornamented surface forms a dull point close to midheight and the margin is concave dorsal to the point (to accommodate the caudal end of the postorbital) and is slanted (rostradorsal to caudoventral) ventral to it (where it is in contact with the jugal). The squamosal overlaps the preopercular and quadratojugal and is overlapped by the postorbital, maxilla and jugal. The dorsal margin of the squamosal lies alongside the postparietal shield of the skull roof and the lateral extrascapular bone and appears not to have an over/underlapping relationship with either. As described above (in section 4.1), the squamosal of *E. wangsjoii* is unique among the species of *Eusthenodon* for the presence of more than one pitline groove, though the condition is unknown in *E. leganihanne*.

The quadratojugal (qj, Figs 2–6, 8, 9) of *E. wangsjoii* is longer than tall with a maximum height just caudal to the bone's midlength. The dorsal margin of the quadratojugal slopes ventrally from the bone's maximum height and the bone is shorter at its rostral end than at its caudal end. It is broadly overlapped dorsally by the preopercular and squamosal bones and so appears very different in its dimensions between dermal (e.g., NHMD 1201204, Fig. 9) and visceral (e.g., NHMD 141689, Fig. 4b) views of articulated cheek specimens. In the isolated right quadratojugal of NHMD 141653, 38% of the height of the bone (in the position of the maximum height dimension) is unornamented overlap zone. The quadratojugal is also overlapped by the maxilla.

The preopercular (pop, Figs 2–5, 8, 9) forms much of the sloping caudal margin of the cheek. Widest near midheight, the preopercular narrows to a blunt point at dorsal and ventral ends where it is overlapped by the squamosal (dorsally) and where it broadly overlaps the quadratojugal (ventrally). None of the specimens in the type series preserve the preopercular in the round and therefore it is impossible to address the nature of the bone's caudal margin, an area that is of potential interest as it has been shown to carry a deep groove interpreted to accommodate the lateral edges of the extrascapular and opercular bones in at least *H. lindae* (Daeschler & Downs 2018).

#### 4.5. Palate

The palate of *E. wangsjoii* is not especially well represented among the type specimens in consideration. Evidence of vomer, parasphenoid, dermopalatine, ectopterygoid and entopterygoid is present, but the bones offer few anatomical details on account of poor preservation and/or limited mechanical preparation. The vomer of *E. wangsjoii* (v, Figs 3, 5) is represented by two specimens, one preserved in visceral view (NHMD 141691) and one in palatal view (NHMD 141653); both of them are highly weathered in such a way that neither allows for detailed description of specific shape characteristics nor surface features. Comparative details among the other two species of *Eusthenodon* are also lacking. Among all of the referred materials of *Eusthenodon bourdoni* and *Eusthenodon leganihanne*, there is only a single partial vomer specimen for *E. bourdoni* (ANSP 23748) that offers incomplete anatomical detail. The vomer of *E. wangsjoii* is observed to exhibit the caudal process that makes for a long

contact with the parasphenoid in some highly nested tristichopterids. In *E. wangsjoii*, the process is especially long, with a parasphenoid contact that extends along ~50% of the total length of the parasphenoid (in NHMD 141653). Among tristichopterids, this is close to the maximum reported relative lengths of the vomer; the vomer–parasphenoid contact is ~55% of total parasphenoid length in *Hyneria lindae* (ANSP 20935C; Daeschler *et al.* 2019) and ~54% of parasphenoid length in *Edenopteron keithcrooki* (ANU V3426; Young *et al.* 2013). The caudal process of the *E. wangsjoii* vomer carries a distinct lateral corner that, in other tristichopterid species, has been shown to be the caudal end of the vomer's visceral articulation site with the entopterygoid. This same corner is observed in *Eusthenopteron jenkinsi* (Downs *et al.* 2018, fig. 3b), *Platycephalichthys bischoffi* (Vorobyeva 1962, plate 9, figs. 2–3), *Langlieria socqueti* (Clement *et al.* 2009, text-fig. 2), *Langlieria radiatus* (Daeschler *et al.* 2019, fig. 7a), *E. keithcrooki* (Young *et al.* 2013, fig. 4) and *H. lindae* (Daeschler & Downs 2018, fig. 6). Rostral to their contact with the parasphenoid, the left and right vomers of *E. wangsjoii* contact one another at the midline, but details of a possible marginal tooth row or sites of contact with premaxilla, maxilla or dermopalatine are not available in the specimens under consideration. In addition to the vomers, NHMD 141653 and 141691 also include parts of the bordering parasphenoid and entopterygoids, and therefore support the interpretation that *E. wangsjoii* did not possess accessory vomers like those observed in several highly nested species of tristichopterid from Australia (*Cabonichthys burnsi*, Ahlberg & Johanson 1997; *E. keithcrooki*, Young *et al.* 2013; and *Mandageria fairfaxi*, Johanson & Ahlberg 1997).

In the one articulated specimen that allows for the measurement (NHMD 141691, Fig. 5b), the width/length ratio of vomers + parasphenoid in *E. wangsjoii* is 0.50. Previous reporting suggested a more narrow medial palate; Daeschler & Downs (2018) reported a width/length ratio of ~0.43 for the vomers + parasphenoid of *E. wangsjoii*, but this was based on a type series specimen that is not considered here to represent the condition in the species (NHMD 153855; see section 2.1). The width/length ratio of vomers + parasphenoid in NHMD 141691 compares favourably with the dimensions in those tristichopterids with relatively wide skulls, including *Langlieria radiatus* (~0.47 in ANSP 21886A; Daeschler *et al.* 2019), *H. lindae* (width/length ratio of ~0.60 in ANSP 20935C; Daeschler & Downs 2018) and *E. keithcrooki* (same ratio is ~0.60 in the skull reconstruction based on ANU V3426; Young *et al.* 2013, fig. 5) and contrasts with the proportions in the uniquely (among highly nested tristichopterids) narrow skull of *M. fairfaxi* (~0.33 in AMF 96855C; Johanson & Ahlberg 1997) and those of more basal tristichopterids including *Heddleichthys dalglesiensis* (~0.35 in BGS 53442; Snitting 2009) and *Eusthenopteron jenkinsi* (0.37 in NUFV 1245; Downs *et al.* 2018). Although two specimens (NHMD 141653, 141691) allow for a length measurement of the parasphenoid bone of *E. wangsjoii* (psp, Figs 3, 5), neither offers any surface detail. Only a single specimen among those in consideration (NHMD 1201211) offers a view of the denticulated surface of the parasphenoid, and this specimen is preserved only in palatal impression. The denticulated surface is observed to be wide (nearly the full width of the parasphenoid bone along part of its length) and with a surface that recesses into the bone. It is therefore similar to the condition observed in *E. bourdoni* (ANSP 25037; Downs *et al.* 2021, fig. 4) and several other highly nested species of tristichopterid (*H. lindae*, ANSP 20935C, Daeschler & Downs 2018, fig. 6a; and *E. keithcrooki*, AMF 134129, Young *et al.* 2019, fig. 8b). The denticulated surface of the *E. wangsjoii* parasphenoid is therefore unlike the wide and 'flat to slightly convex' surface in *E. keithcrooki* (though 'not well preserved' in ANU V3426, Young *et al.* 2013, p. 20,

figs. 4b, 5) and the narrow, raised, keel-like surfaces in all other tristichopterids for which the condition is known. The condition of the parasphenoid is unknown in *E. leganihanne*. In *E. wangsjoii*, the denticulated surface of the parasphenoid appears to be teardrop-shaped with a rounded caudal end and a length that narrows rostrally; the rostral tip is unknown. This is the typical shape among tristichopterids though several species differ; that of *H. dalgleisiensis* is narrow at midlength and widest at rostral and caudal ends ('somewhat hourglass-shaped,' Snitting 2009, p. 280) and that of *E. keithcrooki* is widest at midlength and narrowing both rostrally and caudally (Young *et al.* 2013). Jarvik (1952, plate 12, fig. 4) labels a buccohypophysial foramen (c.hyp. canal for ventral tube of hypophysis) through the caudal end of the parasphenoid's denticulated plate in his figure of NHMD 1201211 (then P. 1482, the aforementioned impression). Because NHMD 1201211 is only an impression of the bone's palatal surface, the specimen is not inconsistent with Jarvik's (1952) interpreted position for the foramen, but new study of this specimen also does not offer evidence in support of the foramen's presence. For comparison, the hypophysial canal of *E. bourdoni* is clearly visible in visceral view of the parasphenoid (ANSP 24502), but no buccohypophysial foramen is observed through the denticulated plate in palatal view (ANSP 25037). Neither of the other two tristichopterid species with a wide, recessed denticulated surface of the parasphenoid preserves evidence of a buccohypophysial foramen penetrating this surface (Young *et al.* 2013; Daeschler & Downs 2018). In the case of *H. lindae*, the hypophysial canal does not pierce the denticulated surface in all four of the well-preserved, well-prepared parasphenoid specimens viewable in the round (ANSP 21461, 23304, 23305, 23306). Jarvik (1952, plate 12, fig. 4) also labels asymmetrically arranged left and right 'posteriorly directed pit[s] of parasphenoid' caudal to the denticulated surface of NHMD 1201211. New study of this specimen suggests that these features are preservational and does not support their identification as anatomical pits.

Only one specimen (NHMD 141653) of *E. wangsjoii* offers partial views of the dermopalatine (dpl, Fig. 3) and ectopterygoid (ect, Fig. 3). The dermopalatine is shown to be distinctly shorter than the ectopterygoid and it carries one fang pair compared to the two in the ectopterygoid. Among tristichopterids within which the condition is known, only *Tristichopterus alatus* (Snitting 2008) and *Timirau clackae* (Swartz 2012) differ by having an ectopterygoid with only one fang pair. A very limited view of the *E. wangsjoii* ectopterygoid (ent, Fig. 3) is possible in only two of the specimens upon which this description is based (NHMD 141653, 141833). Both are preserved in such a way that shape and surface features are impossible to describe. That of NHMD 141653 is preserved in visceral view; that of the holotype is preserved in palatal view but weathered to the point of nearly being a visceral impression.

#### 4.6. Lower jaw

The lower jaw of *E. wangsjoii* is poorly represented among the specimens in the type series. No single complete lower jaw exists but several partially preserved jaws (some primarily [e.g., NHMD 141693] as surface impressions) and isolated dermal bones of the jaw allow for a limited description. The most complete specimens (e.g., NHMD 141833, 153925) reveal the lower jaw to be of the typical shape for a tristichopterid in that it is long, slender and of a low profile. There is a dentary fang pair (d.f, Fig. 3) and the precoronoid fossa is longer than the first intercoronoid fossa. The height of the dentary (d, Figs 2, 3, 6) increases gradually distal to mesial and that of the infradentary series (splenial, spl, Figs 2, 6; postsplenial, pspl, Figs 2, 6; angular, an, Figs 2, 6; and surangular, san, Fig. 6) increases mesial to distal. The ornament of these dermal bones of the labial jaw surface,

with its isolated and conjoined tubercles and short, broken ridges, has a more tuberculate appearance than is observed elsewhere in the dermatocranial skeleton. This is consistent with the conditions in both *Eusthenodon bourdoni* ('an almost tuberculated appearance,' Downs *et al.* 2021, p. 8) and *Eusthenodon leganihanne* ('a more tuberculate appearance than is seen on most of the skull surface,' Downs *et al.* 2023, p. 13).

#### 4.7. Operculogular/extrascapular series

Among the specimens under consideration, the operculogular/extrascapular series of *E. wangsjoii* is represented by opercular (NHMD 141653, 141694), subopercular (NHMD 141691), median and lateral extrascapular (NHMD 141653, 141691, 141833), submandibular (NHMD 141693, 141833) and principal gular bones (NHMD 141693, 141833). The two available opercular bones (op, Figs 3, 7) are differently sized and shaped, but both are taller than they are long. This is the expected condition for a highly nested tristichopterid and differs from the longer than tall opercular bone of *Eusthenopteron foordi* (Jarvik 1944). The larger of the two *E. wangsjoii* specimens (left opercular, NHMD 141653) belongs to an articulated skull. The bone is almost crescent-shaped with a shallow curve to the concave rostral margin and a more deeply curved, convex caudal margin. The shape is atypical among the nearly rectangular-shaped operculars of Tristichopteridae. It is also unusual for having its maximum length in the dorsal half of the bone and narrowing ventrally from this position to the ventral end of the bone. A narrow, depressed, unornamented zone for cheek overlap extends along the rostral margin of the opercular in this specimen. The height-to-length ratio of the NHMD 141653 opercular is 1.93, the highest value for this ratio yet reported among tristichopterids. The second opercular specimen in the *E. wangsjoii* type series (dermal impression, right opercular, NHMD 141694) is preserved in close association with a right cleithrum and partial pectoral fin. Relative to that of NHMD 141653, this opercular exhibits the more typical, nearly rectangular shape with relatively straight rostral and ventral margins and a convexly curving caudal margin (dorsal margin not completely preserved). Its height/length ratio of >1.19 is an underestimate due to its incompletely preserved height; when considering the marked difference in shape between the two opercular bones in the type series, NHMD 141694 is much more likely to be the specimen responsible for the opercular dimensions that have been reported for the species (e.g., a height/length ratio of 1.3 was recently reported by Downs *et al.* 2023). Neither of the two other species of *Eusthenodon* preserves a complete opercular bone; in both, the maximum length of the bone is preserved in each but the maximum height is not, so height/length ratios in these other species are underestimates. The ratio in *Eusthenodon leganihanne* has been calculated as >1.23 (ANSP 21343, Downs *et al.* 2023); that of *Eusthenodon bourdoni* is >1.45 (ANSP 23777).

NHMD 141691 includes a partial dermal impression of an isolated bone inferred to be a subopercular based on shape. One of the bone's margins pinches to form a blunt, rounded point; the rostral margin of the tristichopterid subopercular is known to narrow to such a point where it reaches between the opercular and preopercular bones. The incomplete nature of the bone in this one specimen prevents a more complete description of its shape and contacts.

The median extrascapular of *E. wangsjoii* (m.ex, Figs 2, 3) is represented by two specimens, one preserved in dermal impression (NHMD 141833 [holotype]) and one in dermal view (NHMD 141653). The trapezoid-shaped bone narrows rostrally such that the maximum width of the bone (close to the caudal end) is 2.42 times the width of the rostral margin (NHMD 141653, extrapolation from right side preservation). Because the median extrascapular is broadly overlapped by the lateral

extrascapulars, the rostral width of the bone appears even more narrow in a dermal view of an articulated skull. When overlapped by the lateral bones, the ornamented surface of the *E. wangsjoii* median extrascapular does, however, exhibit enough width along the rostral margin to make for a considerable separation of left from right lateral extrascapular (1.64 cm of separation in the 3.62 cm long median extrascapular of the holotype). It is worthy of note that a wide separation of the lateral extrascapulars was included in Clément's (2002, p. 579) rediagnosis of *Eusthenodon* ('lateral extrascapulars well separated in the midline anteriorly') and is indeed additionally true of *E. bourdoni* (Downs *et al.* 2021, fig. 6b) and *E. leganihanne* (Downs *et al.* 2023, fig. 6). While the lateral extrascapulars may be considered to be 'well separated' in all known *Eusthenodon* material, the character is not included in the revised diagnosis of the present work due to its qualitative nature. The lateral extrascapular of *E. wangsjoii* (1.ex, Figs 2, 5), preserved in only two specimens (in dermal impression, NHMD 141833; and in weathered visceral view, NHMD 141691), allows for only limited description but it is wide (rostral width is 2.5 times the rostral width of the median extrascapular's ornamented surface in NHMD 141833) and heater-shaped (pointed end caudal).

As is typical for a tristichopterid, the principal gular of *E. wangsjoii* (p.g, Figs 2, 6) is rostral–caudally elongate and three-sided, with the longest side bordering the submandibulars, another side bordering the opposite principal gular along the midline, and the third side completing the triangle. The caudo-medial corner is the most rounded and blunt of the three corners. Neither of the two relevant specimens shows evidence of a midline median gular or of a median gular overlap zone on the principal gular, as is observed in *E. foordi* (Jarvik 1944). As expected for a tristichopterid, a series of generally rectangular submandibulars (sm, Figs 2, 6) separates the ventral margin of the lower jaw from the principal gular. In NHMD 141833 (holotype), the left series of nine submandibulars (= branchiostegal rays of Jarvik 1952), and in NHMD 141693, the right series of at least six submandibulars, are preserved in dermal impression. There is no size progression of the submandibulars along the length of the series although the most caudal submandibular is the longest and tallest in the series. In *E. foordi*, the most caudal submandibular is so enlarged and differently shaped relative to the others that Jarvik (1980, Rbr8, fig. 10a, d) inferred it to be a fusion between a submandibular and an opercular bone and referred to it as a submandibulobranchiostegal plate. Though enlarged relative to the others in the series, the most caudal submandibular in *E. wangsjoii* is not oversized or differently shaped to the same degree.

#### 4.8. Pectoral appendicular bones

Among the type series of specimens, the appendicular skeleton of *E. wangsjoii* is represented by two cleithra (one right, NHMD 141653B, one left, 141694), possible pectoral fin mesomeres and radials (NHMD 141653, 141833) and an isolated possible fin radial (NHMD 141689). The two cleithrum specimens are both preserved in visceral view and are incomplete ventrally; as a result, they do not allow for description of the dermal ornament nor of the bone's relationships with the clavicle and the scapulocoracoid. The cleithrum of *E. wangsjoii* has the typical boomerang shape with a long dorsal lamina that bends away from a ventral lamina. The dorsal lamina of the *E. wangsjoii* cleithrum is gently curved along both cranial and caudal margins and it maintains a nearly constant width along its entire height. The dorsal end of the lamina is bluntly rounded. The cleithrum of NHMD 141694 (cl, Fig. 7) shows the bone to widen ventrally at the transition to the ventral lamina, giving the caudoventral corner a heeled appearance. The cleithrum of NHMD 141694

is associated with fragmentary evidence of the pectoral fin including lepidotrichia, fin scales and potential mesomeres and/or radials. NHMD 141653 (Fig. 3a) includes fin scales, lepidotrichia and mesomeres of the left pectoral fin. The only potential mesomere complete enough to be described is a possible third mesomere (= ulnare, ulr?, Fig. 3). The tristichopterid ulnare conforms in general shape to the bone seen in NHMD 141653, with its postaxial blade and its parallel contact surfaces for second mesomere (= ulna) at the proximal end and fourth mesomere at the distal end. Impressions of a possible mesomere and a preaxial radial of the pectoral fin are associated with the holotype specimen (NHMD 14833). The possible mesomere has a slight hourglass shape and appears to carry a single site of contact on one articulating end and two on the opposite; these shape characteristics match those of the fourth mesomere in the tristichopterid pectoral fin. The possible preaxial pectoral radial has a pronounced hourglass shape, much wider at both ends than at midlength. NHMD 141689 includes a possible pectoral fin radial in isolation. One of the articulating ends is blunt; preservation does not allow for a more complete description.

#### 4.9. Scales

Scales associated with several specimens in the *E. wangsjoii* type series (NHMD 141689, Fig. 4c; NHMD 141691) inform the condition for the species. The scales of *E. wangsjoii* are thin, circular/ovoid (long dimension cranial–caudal in some, orthogonal to axis in others) to waisted, and without a cosmine layer. The piri-form (pointed end rostral), protruding boss on the visceral surface of the scale contributes to the diagnosis of Tristichopteridae. Most scales are 2–3 cm long. The waisted scales have an exposed, ornamented portion that is offset from the main scale body by a pinched margin (the waist). Among the observable examples, the height of the ornamented surface (caudal to the waist) is less than the height of the main body of the scale (cranial to the waist). In several instances, the condition matches that of *Eusthenodon bourdoni* (Downs *et al.* 2021, fig. 7) in that the waist is more like a narrowing of the scale between its overlapped and exposed portions as the ornamented part of the scale does not expand in height caudal to the waist but does protrude caudally from the outline of the main scale body. Among tristichopterid species, scales with a pinched waist are not common but have additionally been reported in *Mandageria fairfaxi* ('ornamented area [...] offset by a "waist"; Johanson & Ahlberg 1997, p. 64), *Langlieria smalingi* ('caudal expansion is offset from the rest of the scale by a [...] pinched waist,' Downs & Daeschler 2022, p. 252) and *Hynieria udlezinye* (Gess & Ahlberg 2023, fig. 12b). In *E. wangsjoii*, as in both other species of *Eusthenodon*, there is an especially high degree of overlap among the scales; in the most extreme examples, the ornamented, exposed portion of the scale comprises only about one-quarter of the scale's total dermal surface area.

The ornamented surface of *E. wangsjoii* scales (Fig. 4c) comprises a dense collection of conjoined tubercles and straight to sinuous ridges with the ridges following a slightly radiating rostral to caudal directionality. The scale ornament is visually consistent with that of the two other species of *Eusthenodon*: *E. bourdoni* (where scale ornament was described as 'conjoined pustules', Downs *et al.* 2021, p. 10, fig. 7a) and *Eusthenodon leganihanne* ('tuberous with conjoined tubercles and irregular broken ridges,' Downs *et al.* 2023, p. 15, fig. 9). The scales of the *E. wangsjoii* type series do not exhibit incised grooves in the ornamented surface, as are common among tristichopterid species, whether tightly spaced (space between adjacent grooves approximately as wide as a groove) as in the scales of *Langlieria radiatus* (Daeschler *et al.* 2019, fig. 11a), *L. smalingi* (Downs & Daeschler 2022, fig. 7c) and *M. fairfaxi*; or widely spaced (space between grooves much wider than a groove) as in *E. leganihanne*

(Downs *et al.* 2023, fig. 9b), *Edenopteron keithcooki* (Young *et al.* 2013, p. 27, fig. 20c) and *Cabonichthys burnsi* (Ahlberg & Johanson 1997, p. 662; Young 2008, fig. 4b). Several weathered tristichopterid scales, preserved in visceral view, from the Britta Dal Formation (e.g., NHMD 154652), show sediment-filled, linear, tightly spaced, radiating features that appear more likely to be internal tubules than incised grooves in the dermal surface. Widely spaced, radiating, incised grooves are observed among the tristichopterid scales from the Hunter Sandstone (upper Famennian, Grenfell, New South Wales, Australia) that were originally assigned to ‘*Eusthenodon gavini*’ (Johanson & Ritchie 2000), later to *Eusthenodon cf. wangsjoii* (Johanson 2004), and most recently to *cf. Eusthenodon* sp. indet. (Downs *et al.* 2023).

## 5. Results

### 5.1. Phylogenetic analysis

The branch-and-bound search resulted in 1,002 most parsimonious trees (MPTs; supplementary File 4) with a tree length (L) of 58 steps (consistency index [CI] = 0.517, retention index [RI] = 0.702, rescaled consistency index [RCI] = 0.363). The strict (SCT; L = 80, CI = 0.375, RI = 0.468, RCI = 0.176) and 50% majority-rule (MRCT; L = 59, CI = 0.509, RI = 0.692, RCI = 0.352) consensus trees of all MPTs (L = 58, CI = 0.517, RI = 0.696, RCI = 0.360) are shown in Fig. 13. Bremer values are low at all nodes (1 for all resolved clades of the consensus trees) so the hypothesised relationships decay quickly when more than the most parsimonious trees are considered in the consensus analysis. In both consensus trees, *Tristichopterus alatus* belongs to a basal polytomy with the two chosen outgroups *Gogoniasus andrewsae* and *Spodichthys buetleri*. In both consensus trees, *Eusthenopteron foordi* is the sister group to *Eusthenopteron wenjukowi* + all higher tristichopterids (nodes 15 and 21). Both consensus trees resolve sister group relationships between *Tinirau clackae* and *Hyneria udlezinye* (nodes 10 and 18), between *Platycephalichthys bischoffi* and *T. clackae* + *H. udlezinye* (nodes 11 and 19) and between *Edenopteron keithcooki* and *Eusthenodon leganihanne* (nodes 3 and 16, and consistent with the results of Downs *et al.* 2023).

The MRCT of this analysis resolves nine relationships that are not found in the SCT: *Eusthenopteron jenkinsi* + all higher tristichopterids (node 13, recovered in 66% of MPTs); (*P. bischoffi* + (*T. clackae* + *H. udlezinye*)) + all higher tristichopterids (node 12, recovered in 76% of MPTs); *Notorhizodon mackelveyi* + all higher tristichopterids (node 9, recovered in 56% of MPTs); *Heddleichthys dalgleisiensis* + all higher tristichopterids (node 8, recovered in 62% of MPTs); *Cabonichthys burnsi* + all higher tristichopterids (node 7, recovered in 99% of MPTs); *Langlieria socqueti* + all higher tristichopterids (node 6, recovered in 66% of MPTs); *Eusthenodon bourdoni* + all higher tristichopterids (node 5, recovered in 91% of MPTs); a polytomous relationship among *Hyneria lindae*, *E. wangsjoii* and *Mandageria fairfaxi* + *Langlieria smalingi* + *Langlieria radiatus* (node 2, recovered in 77% of MPTs); and the polytomous relationship among *M. fairfaxi*, *L. smalingi* and *L. radiatus* (node 1, recovered in 57% of MPTs). The character state changes that unambiguously map to the nodes of the MRCT are communicated in full in the caption to Fig. 13.

## 6. Discussion

### 6.1. Phylogenetic analysis

The 50% majority rule consensus tree (MRCT; Fig. 13) resolves many of the tristichopterid relationships previously hypothesised by other recent phylogenetic assessments of Tristichopteroidea

(Olive *et al.* 2020; Downs & Daeschler 2022; Downs *et al.* 2023). *Mandageria fairfaxi*, *Langlieria smalingi* and *Langlieria radiatus* form a polytomous clade of species in the MRCTs of Downs & Daeschler (2022), Downs *et al.* (2023) and in that of the present work (node 1). *Eusthenodon leganihanne* and *Edenopteron keithcooki* are sister species in the MRCT of Downs *et al.* (2023) and in that of the present work (node 3). *Eusthenodon wangsjoii*, *E. leganihanne*, *E. keithcooki*, *Hyneria lindae*, *L. smalingi*, *L. radiatus* and *M. fairfaxi* comprise a clade of tristichopterids in the MRCT of the present work (node 4); this same clade appears in the MRCTs of Downs & Daeschler (2022) and Downs *et al.* (2023) but for the exclusion of *E. leganihanne* in Downs & Daeschler (2022), a species that had not yet been described. The species of *Hyneria* and *Edenopteron* were not included in phylogenetic analyses prior to that of Olive *et al.* (2020), but the new analysis continues a tradition of support for a highly nested clade of tristichopterids that variably includes *H. lindae* and the species of *Cabonichthys*, *Edenopteron*, *Eusthenodon*, *Hyneria*, *Langlieria* and *Mandageria* (e.g., Ahlberg & Johanson 1997, 1998; Johanson & Ahlberg 2001; Zhu & Ahlberg 2004; Snitting 2008; Clément *et al.* 2009; Swartz 2012; Olive *et al.* 2020; Downs *et al.* 2021, 2023). This clade was labelled the ‘Famennian clade’ by Olive *et al.* (2020, p. 11) and while it did include only Famennian species, it was forced to leave one out due to unresolved relationships among *Heddleichthys dalgleisiensis* and several Frasnian species. In the MRCT of the present work (and in those of Downs & Daeschler 2022 and Downs *et al.* 2023), the clade that originates at the most recent common ancestor of all Famennian species (node 8) includes a single Frasnian species in *Langlieria smalingi*. Following the precedent of Downs & Daeschler (2022) and Downs *et al.* (2023), I use the term ‘highly nested tristichopterids’ when referring to the members of this clade.

In the MRCT of Downs *et al.* (2023), the polytomous clade that includes *M. fairfaxi*, *L. smalingi* and *L. radiatus* was sister to *H. lindae*. Here it belongs to a more inclusive polytomy that additionally includes *H. lindae* and *E. wangsjoii* (node 2, recovered in 77% of MPTs). The new scoring of *E. wangsjoii*, along with the other changes made to the character data of Downs *et al.* (2023; supplementary File 1), has moved the species to a more highly nested position in the tristichopterid cladogram. In the MRCT of Downs *et al.* (2023), *E. wangsjoii* appeared as sister species to (*E. leganihanne* + *E. keithcooki*) + (*H. lindae* + (*M. fairfaxi* + *L. smalingi* + *L. radiatus*)). A highly nested position for *E. wangsjoii* was anticipated by derived anatomical features in the species. These include postorbital exclusion from the orbital margin (unambiguously mapped to node 20, Fig. 13), a teardrop-shaped pineal series (node 20) in a position well caudal to the orbits (nodes 14, 20), two fang pairs of the ectopterygoid (node 15 [ACCTRAN], node 9 [DELTRAN]), a dentary fang pair (nodes 12, 20), and a denticulated field of the parasphenoid that is recessed into the body of the bone (node 5). According to the results of the new analysis, and those of Downs & Daeschler (2022) and Downs *et al.* (2023), *Eusthenodon* is not monophyletic, nor are any of the multi-specific tristichopterid praenomina (including additionally *Eusthenopteron*, *Langlieria* and *Hyneria*). *Eusthenopteron* is paraphyletic according to our results; the three others are polyphyletic. Of course, phylogenetic results do not dictate praenomen assignments; all of the affected species were appropriately assigned a praenomen according to prevailing published diagnoses. Our phylogenetic results do not (nor do any phylogenetic results) challenge the binomials of any of the species belonging to paraphyletic or polyphyletic praenomina. Despite its rampant practice in palaeontology especially, there exists no widely accepted taxonomic code that supports changing a species binomial in response to phylogenetic results. Because the species

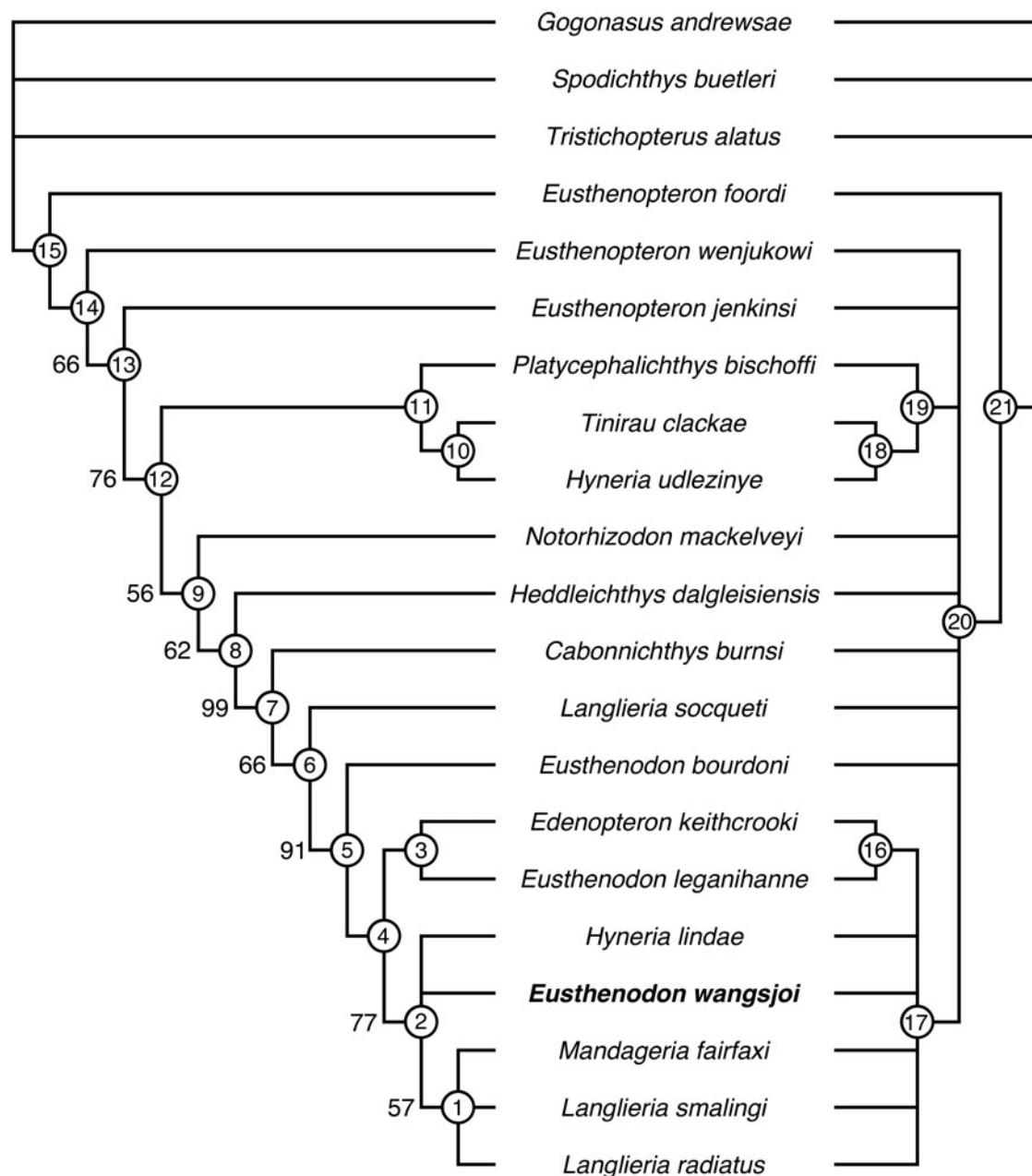


**Figure 13** The 50% majority-rule consensus tree (MRCT, left) and strict consensus tree (SCT, right) obtained in the maximum parsimony analysis that resulted in 1,002 most parsimonious trees (MPTs) of 58 steps each (MRCT values: L = 59, CI = 0.509, RI = 0.692, RCI = 0.352; SCT values: L = 80, CI = 0.375, RI = 0.468, RCI = 0.176). The 21 circled nodes were arbitrarily assigned numbers and those numbers are referenced in the text. The numerical values that label the nodes outside the circles are the frequency of occurrence of that node among the 1,002 MPTs. All nodes without such labels appear in 100% of the MPTs. The term 'highly nested', as used in the text, refers to all of the species that belong to the clade at nodes 8 (of the MRCT). Each of the following character state changes unambiguously maps (in both ACCTRAN + DELTRAN optimisations) to the listed node using the notation 'node #: (character) #, (state before change) # → (state after change) #': node 1: 20, 1→0; 27, 0→1; node 2: 23, 1→0; node 3, 6, 1→0; 27, 0→2; node 4: 3, 0→1; 5, 0→1; node 5: 20, 0→1; node 6: 18, 1→0; node 7: 13, 0→1; 15, 0→1; 24, 0→2; node 10: 25, 1→0; node 11: 11, 1→0; node 12: 17, 0→1; node 14: 6, 0→1; 8, 0→1; node 15: 11, 0→1; 12, 0→1; 19, 0→1; 21, 0→1; node 16: 6, 1→0; 13, 0→1; 25, 0→1; 27, 0→2; 1→0; node 17: 1, 0→1; 3, 0→1; 5, 0→1; 18, 1→0; 21, 1→0; 23, 1→0; 24, 0→2; 25, 1→0; 26, 0→1; node 18: 25, 1→0; node 19: 11, 1→0; 18, 1→0; node 20: 2, 0→1; 4, 0→1; 6, 0→1; 7, 0→1; 8, 0→1; 9, 1→2; 17, 0→1; 23, 0→1; node 21, 0→1; 11, 0→1; 12, 0→1; 19, 0→1; 21, 0→1.

praenomen explicitly does not carry any implication of monophyly (de Queiroz & Cantino 2020), phylogenetic results hold no influence over its usage.

## 6.2. Description of additional NHMD specimens that potentially represent *Eusthenodon wangsjoii*

Collecting at the Britta Dal Formation exposures on Gauss Halvø and Ymer Ø (Fig. 1) has recovered numerous fossils, most of them previously unreported, that compare favourably with the condition in *E. wangsjoii* but did not contribute to the species description of section 4 for the reasons presented in section 2.1. With the

recognition that there are at least two Britta Dal tristichopterid species, I hesitate to assign any specimen to *E. wangsjoii* if it lacks the features or associations needed to make the assignment. As a result, with the exception of NHMD 153855 (*E. wangsjoii* paratype), the NHMD specimens presented here in this section are all assigned to cf. *E. wangsjoii*. I provide brief anatomical descriptions as a way of sharing the remainder of the relevant inventory of fossils at the NHMD that reflect decades of collecting efforts in East Greenland's Britta Dal Formation. Isolated tristichopterid type scales are common in the Britta Dal Formation and will not be reported here.

**6.2.1. Articulated skulls.** NHMD 1201214 (Fig. 14a), an East Greenland specimen without specific locality or stratigraphic information, is an articulated tristichopterid skull roof (preserved partly in visceral impression and partly in dermal view), the associated left cheek (visceral impression) and lateral extrascapular (dermal view). The exposed dermal ornament comprises isolated and conjoined tubercles and is without the anastomosing ridges that are common in *E. wangsjoii*. At 15.6 cm in total length, the skull roof is small relative to the *E. wangsjoii* holotype (and indeed all of those in the type series with the exception of NHMD 153855, a skull that is described below but was eliminated from consideration in the *E. wangsjoii* species description of section 4; see section 2.1 for rationale). The length ratio of parietal shield to postparietal shield is 1.93, a value that is outside (less than) the range of values calculated for the other relevant specimens in the type series and is also lower than the values calculated for the two other species of *Eusthenodon*. The width/length ratio of the parietal shield is 0.62, a value that is outside (greater than) the range calculated for the other relevant specimens in the type series and for the other species of *Eusthenodon*. This suggests a shorter, blunter snout than is described for *E. wangsjoii*. The length of the parietal bones of NHMD 1201214 is 72 % of parietal shield length in visceral view. The rostral margin of the parietal reaches 4 mm rostral to the orbital margin, again in visceral view; no specimen of *E. wangsjoii* has a parietal reach rostral to the orbit, but within the type series of specimens the relationship may only be assessed in dermal view; overlap of nasals onto the rostral parietal makes for a shorter parietal in dermal than in visceral view. The parietal bone of NHMD 1201214 is wide (width/length ratio = 0.44) relative to those in the three largest skulls in the *E. wangsjoii* type series, but within the range of values for this ratio among all relevant specimens of the *E. wangsjoii* type series. The median postrostral and surrounding nasal bones are visible in NHMD 1201214 but specific shapes and counts (of nasals) are impossible to assess. The pineal series is in the shape of a minor circular sector, with the rounded end rostral and pointed end caudal. It is located entirely caudal to the rostral reach of the intertemporal bones. A large, circular pineal foramen is visible in at least the visceral view provided by this portion of the specimen. In visceral view, the long intertemporal is widest at its caudal end and it narrows to a rostral point; it does not exhibit visceral contact with the posterior supraorbital. The width/length ratio of the postparietal shield is 1.67, within the range determined for *E. wangsjoii*. The postparietal bone is similarly shaped to that of *E. wangsjoii*, with caudal width much greater than rostral width (ratio of 2.5 for the left postparietal; 1.88 for the right). The supratemporal forms a distinctly rounded, lobate rostrolateral process that, like that of *E. wangsjoii*, reaches rostral to the postparietal bone's rostral margin. The orbital margin of the posterior supraorbital is longer than the bone's caudal process, counter to the condition in *E. wangsjoii*. Lacrimal, jugal, postorbital, squamosal and preopercular bones are all well observed in the specimen; only part of the dorsal edges of the maxilla and quadratojugal are exposed. Specimen preservation (ventrally incomplete visceral impression) does not allow for description of the nature of the relationships among the bones of the cheek nor of relevant characteristics like the position of the maxilla's maximum height or the percentage of lacrimal length rostral to the orbit. The jugal is rectangular, and longer than tall. The tall caudodorsal point of the lacrimal is similar to that of *E. wangsjoii*, and like the condition in that species, it contacts the posterior supraorbital and restricts the jugal and postorbital from the orbital margin. The one preserved (left) lateral extrascapular is preserved in dermal view and of minor circular sector shape, pointed end rostrolateral.

NHMD 153855 (Fig. 14b–e) is a series of impressions of a nearly complete skull (including skull roof [dermal and visceral

impressions], cheeks [dermal impression], palate [dermal and visceral impressions], operculogular bones [visceral impression] and lower jaws [matrix cast] in seven total pieces) from Sederholm Bjerg on Gauss Halvø. The specimen belongs to the *E. wangsjoii* type series but is of a markedly different size scale from the others (skull roof length = 8.46 cm) and was therefore excluded from consideration by the species description of section 4 (see section 2.1 for rationale). The dermatocranial ornament is a finely reticulating pattern with pitline grooves observed on the parietal (short and arching, concave caudolateral), tabular (arching, concave caudal) and postparietal (transversely oriented). The length ratio of parietal shield to postparietal shield is 2.00, which is just below the range of values calculated for the other specimens in the type series that allow the calculation. The width/length ratio of the parietal shield is 0.70, a value that is outside (greater than) the range calculated for the other specimens in the type series and for the other species of *Eusthenodon*. This suggests a shorter, blunter snout than is described for *E. wangsjoii*. In comparison to the other specimens in the type series, the parietal bones of NHMD 153855 are short (65 % of parietal shield length in visceral view) and do not reach rostrally beyond the orbit in dermal view. The parietals are also relatively narrow with a width/length ratio (0.29) that falls outside (is lower than) the range of values calculated for the other type specimens. The median postrostral of NHMD 153855 is a large bone (66 % of the parietal bone length in dermal, articulated view) that is bordered laterally by an indeterminate number of nasal bones (only the borders of the most caudal may be discerned). The pineal series is teardrop-shaped (pointed end caudal) and its rostral margin nearly aligns with the rostral tip of the intertemporal in dermal view. A small, circular pineal foramen through dermal and visceral surfaces is visible at the caudal end of the series. The intertemporal is a long and narrow bone that narrows to a rostral point. Whether it contacts the posterior supraorbital is impossible to determine. The postparietal shield is wider than long, with a width/length ratio (1.71, extrapolation from right side preservation) that is within the range of values calculated for *E. wangsjoii*. The caudal width of the postparietal bone is 2.2 times the rostral width, a value that is also consistent with the condition described for *E. wangsjoii*. The supratemporal bone of NHMD 153855 has a short rostral lobe that extends beyond the postparietal bone's rostral margin, and a long, caudally sloping rostrolateral margin. It forms the rostral part of the postparietal shield's shallow lateral notch. Beyond the two supraorbital bones, it may not be determined which bones contribute to the orbital margin. All that may be observed of the cheek skeleton are partial impressions of the left and right squamosals and postorbitals, and the left jugal and possibly preopercular. The palate includes views of the parasphenoid, vomers, entopterygoid, dermopalatine and ectopterygoid in visceral impression, and the parasphenoid and entopterygoid in dermal impression. The caudal process of the vomer is relatively short; 34 % of parasphenoid length is in contact with the vomer, while greater than 50 % of parasphenoid length contacts the vomer in the other specimens in the *E. wangsjoii* type series. The dermopalatine of NHMD 153855 is considerably longer than the ectopterygoid (at least in visceral articulated view), counter to the condition in the one other relevant specimen in the *E. wangsjoii* type series (NHMD 141653). The denticulated field of the parasphenoid is wide and recessed into the bone. The lower jaw natural casts and the visceral impressions of the submandibulars do not offer any describable anatomy. The shape of the principal gulars matches the condition described for *E. wangsjoii*.

NHMD 142051 (Fig. 14f) from Kerstin Dal on Gauss Halvø includes a partial parietal shield and a partial postparietal shield. The partial parietal shield is preserved in visceral view and includes the median postrostral, right anterior supraorbital,

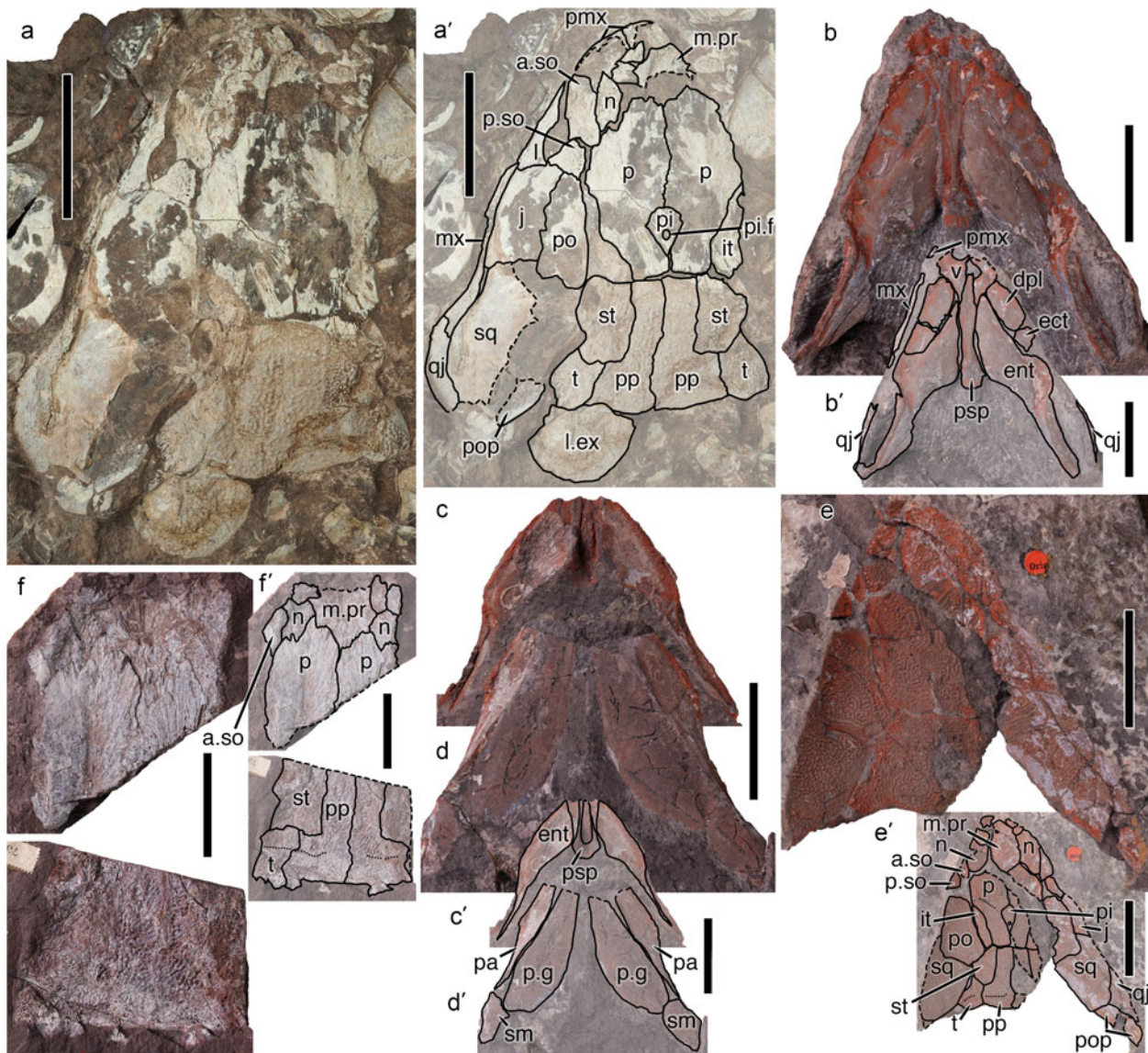


**Figure 14** (a) cf. *E. wangsjoii*, NHMD 1201214, skull roof and left cheek primarily in visceral impression (a, photograph; a', labelled illustration); (b–e) *E. wangsjoii*, NHMD 153855: (b) dermal bones of the palate in visceral impression (b, photograph; b', labelled illustration); (c) dermal bones of the palate in dermal impression (c, photograph; c', labelled illustration); (d) prearticulars and bones of the operculogular series in visceral impression (d, photograph; d', labelled illustration); (e) skull in dermal impression (e, photograph; e', labelled illustration); (f) cf. *E. wangsjoii*, NHMD 142051, parietal shield in visceral view and postparietal shield primarily in dermal impression (f, photograph; f', labelled illustration). Dotted lines follow pitline grooves; dashed lines follow unfinished bone margins. Abbreviations: a.so = anterior supraorbital; a.t = anterior tectal; dpl = dermopalatine; ent = entopterygoid; ect = ectopterygoid; it = intertemporal; j = jugal; l = lacrimal; l.ex = lateral extrascapular; m.pr = median postrostral; mx = maxilla; n = nasal; p = parietal; pa = prearticular; p.g = principal gular; pi = pineal bones; pi.f = pineal foramen; pmx = premaxilla; po = postorbital; pop = preopercular; pp = postparietal; p.so = posterior supraorbital; psp = parasphenoid; qj = quadratojugal; sm = submandibular; sq = squamosal; st = supratemporal; t = tabular; v = vomer. Scale bars of (a) and (f) equal 5 cm; scale bars of (b–e) equal 3 cm.

part of the nasal series and the rostral ends of the parietals. It offers little describable anatomy but a parietal width of 5.3 cm helps to communicate scale. The postparietal shield of the same specimen is preserved in dermal impression. The dermal ornament is more tuberculate (isolated and conjoined tubercles) than that which is common in *E. wangsjoii*. The rostral end of the postparietal shield is missing so relevant shape characteristics of the shield and postparietal bone are impossible to quantify. The qualitative shapes of the three bones in the shield match the general expectations set by *E. wangsjoii*. The supratemporal flares laterally and borders the shallow lateral notch of the postparietal shield. A nearly transverse pitline groove is continuous across the tabular and caudal end of the postparietal bones. Postparietal and tabular bones carry an unornamented zone, along the caudal margin, that probably accommodated the overlapping bones of the extrascapular series.

NHMD 152611 (Fig. 15a) from Smith Woodward Bjerg on Gauss Halvø is a partial parietal shield (including median postrostral, part of the left nasal series, left anterior and posterior supraorbitals, partial left parietal and left intertemporal), partial postparietal shield (without discernible details), left cheek (including lacrimal, jugal and postorbital) and partial extrascapular series, preserved entirely in dermal impression. The median postrostral is proportionally large relative to the condition in *E. wangsjoii*; the bone is incomplete rostrally but even the length of the preserved portion alone is 67% of the length of the parietal bone (though incomplete caudally, the maximum parietal length is inferred from the position of the parietal shield's caudal margin). The specimen therefore bears a strong similarity to the short, wide, postrostral and pineal dominated skull roofs (NHMD 1201203, 1201216) that Jarvik (1985) assigned to *E. wangsjoii*, but which are considered cf. *E. wangsjoii* here and

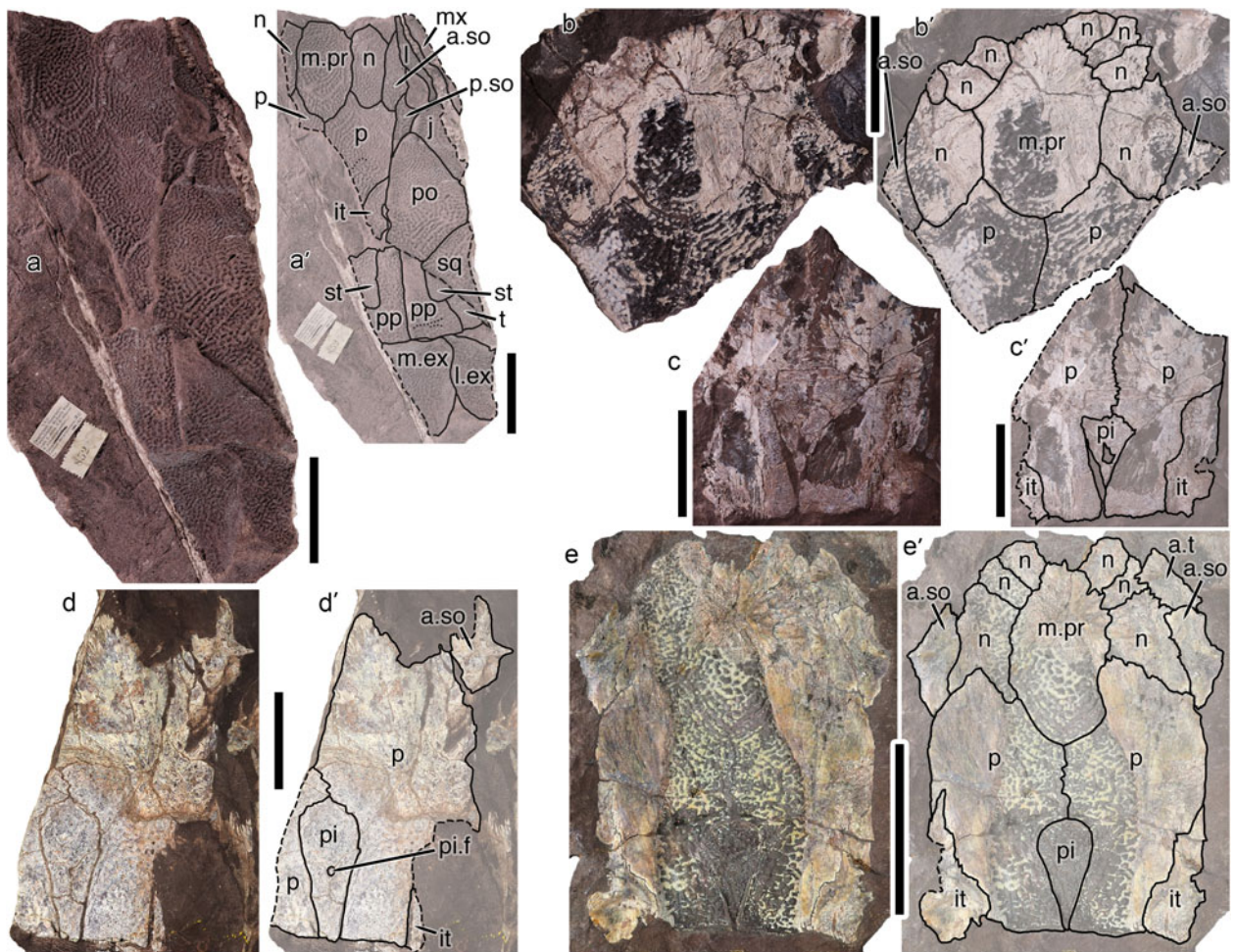


**Figure 15** cf. *E. wangsjoii*. (a) NHMD 152611, skull roof, left cheek and extrascapular bones in dermal impression (a, photograph; a', labelled illustration); (b) NHMD 141667, partial parietal shield in visceral view and dermal impression (b, photograph; b', labelled illustration); (c) NHMD 154696, partial parietal shield primarily in visceral impression (c, photograph; c', labelled illustration); (d) NHMD 1201216, partial parietal shield in weathered dermal view (d, photograph; d', labelled illustration); (e) NHMD 1201203, parietal shield in visceral view and dermal impression (e, photograph; e', labelled illustration). Dotted lines follow pitline grooves; dashed lines follow unfinished bone margins. Abbreviations: a.so = anterior supraorbital; a.t = anterior tectal; it = intertemporal; j = jugal; l = lacrimal; l.ex = lateral extrascapular; m.ex = median extrascapular; m.pr = median postrostral; n = nasal; p = parietal; pi = pineal bones; pi.f = pineal foramen; po = postorbital; pp = postparietal; p.so = posterior supraorbital; sq = squamosal; st = supra-temporal; t = tabular. Scale bars of (a), (c) and (e) equal 5 cm; scale bars of (b) and (d) equal 3 cm.

are described later in this section. The pineal series of NHMD 152611 is not preserved to support the comparison. The dermato-cranial ornament compares favourably with that of *E. wangsjoii*. A short section of the posterior oblique pitline groove is observed on the parietal and the preserved section is entirely rostral to the intertemporal. The intertemporal is long and narrows to a rostral point. The posterior supraorbital exhibits a pointed caudal process that is longer than the bone's orbital margin but does not reach the rostral tip of the intertemporal, at least in dermal view. The entire left orbital margin of NHMD 152611 is preserved; lacrimal and posterior supraorbital do not contact, allowing the jugal to contribute to the margin. This is unlike the condition in *E. wangsjoii* (where only the supraorbitals and lacrimal form the orbit), but is similar to the condition in *Eusthenodon bourdoni*, an *Eusthenodon* species partly diagnosed by the jugal's contribution to the orbit (Downs *et al.* 2021). The preserved portions of the median and left lateral extrascapular of NHMD 152611 match the general shape expectations set by *E. wangsjoii*.

**6.2.2. Parietal shields.** NHMD 141667 (Fig. 15b) from Sederholm Bjerg on Gauss Halvø is a small partial parietal shield partly preserved in visceral view and partly in dermal impression. The specimen includes the median postrostral, partial anterior supraorbitals, a nasal series that includes at least four

nasals on one side (the largest of which is most caudal) and the rostral ends of the parietals. The dermal ornament is observed to be similar to that of *E. wangsjoii* with tubercles and anastomosing ridges. NHMD 154696 (Fig. 15c) from Kerstin Dal is a partial parietal shield preserved primarily in visceral impression. Only partial parietal bones, left intertemporal and the pineal series are preserved. The pineal series is triangular in shape (symmetrical across the midline and with one corner pointed caudal) and is pierced by a large foramen near to its caudal tip. The intertemporals are long and narrow.

NHMD 1201216 (Fig. 15d) from Celsius Bjerg on Ymer Ø and NHMD 1201203 (Fig. 15e) from Smith Woodward Bjerg on Gauss Halvø are the two similarly short and wide parietal shield specimens that Jarvik (1985, p. 48) assigned to *E. wangsjoii* but recognised to be 'extreme variants' on the condition observed in the species, and for which he entertained the possibility that 'more than one species is involved'. NHMD 1201203 (preserved partly in visceral view and partly in dermal impression) is the more complete of the two, missing only the most rostral end of the shield; NHMD 1201216 (preserved in weathered dermal view) includes only the left anterior supraorbital, left parietal, the pineal series and fragments of the left intertemporal and right parietal. The width/length ratio of the parietal shield of NHMD 1201203 is ~0.81 (a shape

extrapolation due to missing rostral end), a value well outside the range calculated for *E. wangsjoii* where the maximum value is 0.56 (in the proportionally widest skull, NHMD 153925). The parietal bone of NHMD 1201203 is also relatively wide (width/length ratio of ~0.52) but near to the condition in the smallest specimen considered by the *E. wangsjoii* description of section 4 (same ratio is 0.53 in NHMD 1201222). The length ratio of parietal bone to parietal shield in NHMD 1201203 (~0.65) also falls within the range measured in *E. wangsjoii*. In NHMD 1201203, the median postrostral (length is 71 % of parietal length in dermal view) and pineal series (length is 43 % of parietal length in dermal view) are especially large relative to the condition in *E. wangsjoii*. The teardrop-shaped pineal series (in dermal view) is nearly as long as the intertemporal bone (in visceral view) and contributes to the caudal margin of the parietal shield. No pineal foramen may be discerned through the dermal surface. The intertemporals are long and narrow rostrally; posterior supraorbital bones are missing so it is unknown if they contacted the intertemporal. The nasal series includes at least three nasal bones on a single side. NHMD 1201216 is much less complete than NHMD 1201203, but it too possesses an especially large pineal series. In this specimen, the pineal series is rounded at its rostral end, narrows caudally, but has a flat transverse caudal end where it makes a considerable contribution to the caudal margin of the parietal shield. A small, circular pineal foramen appears at approximately midlength.

**6.2.3. Postparietal shields.** NHMD 141750 (Fig. 16a) from Kerstin Dal is a small (5.05 cm in length) left side postparietal shield preserved in weathered dermal view. The dermatocranial ornament is difficult to assess in full but it appears generally consistent with the condition in *E. wangsjoii*. The width/length ratio of the entire shield is 1.45 (extrapolation from left side preservation), within and near to the narrow end of the range of values calculated for *E. wangsjoii*. As in *E. wangsjoii*, the caudal width of the postparietal bone is more than double (2.13 times) the bone's rostral width. The supratemporal has a minor rostralateral flange; the ornamented surface has a long, curved (concave) rostralateral margin with an overlap zone to accommodate the postorbital. The supratemporal and tabular form the shallow lateral notch of the postparietal shield. The weathered dermal surface obscures any potential pitline grooves.

NHMD 141999 (Fig. 16b) from Smith Woodward Bjerg includes a small (5.93 cm in length), complete postparietal shield preserved partly in weathered visceral view and partly in dermal impression; it additionally includes potential infradentaries that are described below. The dermatocranial ornament of the postparietal shield is like that of *E. wangsjoii*. The width/length ratio of the entire shield is 1.80, within and near to the wider end of the range of values calculated for *E. wangsjoii*. The caudal width of the postparietal bone is more than double (2.73 times) the bone's rostral width. The rostralateral flange of the supratemporal forms the rostral margin of the postparietal shield's lateral notch. The sections of dermal preservation do not allow for assessment of potential pitline grooves.

**6.2.4. Cheek bones.** NHMD 141669 (Fig. 17a) from Kerstin Dal is a partial, articulated left cheek specimen preserved in dermal view; it includes the complete lacrimal, partial jugal and fragments of maxilla. The dermatocranial ornament is consistent with the condition in *E. wangsjoii*. The lacrimal's orbital margin suggests a lenticular shape to the orbit (long dimension caudodorsal to rostroventral). The posterior supraorbital is not preserved, so whether the jugal reached the orbital margin in this individual is unknown. Unlike the condition in the one relevant specimen of *E. wangsjoii* (NHMD 153925), less than half of the lacrimal's length is rostral to the orbit (27 % of total length compared to 56 % in NHMD 153925). The maxilla is incomplete ventrally but the dorsal margin has peaks both at the

lacrimal–jugal and the jugal–squamosal contacts. NHMD 154652 from Smith Woodward Bjerg preserves the right lacrimal and fragments of the associated jugal and maxilla, in visceral view (in addition to an entopterygoid and anocleithrum described below). Less than half of lacrimal length (25 %) is rostral to the lenticular orbital margin. The maxilla, here preserving part of its row of labyrinthodont teeth, has a dorsal peak at the lacrimal–jugal contact. NHMD 154656 from Smith Woodward Bjerg includes a rostral end fragment of a maxilla preserved in weathered visceral view; labyrinthodont teeth are observed. This same specimen additionally includes a left squamosal partly in visceral view and partly in dermal impression. The dermatocranial ornament matches the condition in *E. wangsjoii*.

NHMD 1201206 (P. 1693 of Jarvik 1985; Fig. 17b) from Celsius Bjerg is a dermal impression of a left maxilla that Jarvik (1985, fig. 37c) assigned to *E. wangsjoii* and used to support his reporting that the bone in the species is tallest in the rostral half. Were this to be true, it would be unique among all known tristichopterid species. New study of the specimen reveals that, in the position of the jugal–squamosal contact, and for much of its caudal half, NHMD 1201206 is incompletely preserved ventrally (Fig. 17b). If complete, the bone would be taller than it appears at the jugal–squamosal contact, making maxillary height in the specimen no greater in the rostral than in the caudal half, whether measuring total bone height or height of only the ornamented, non-overlapped, surface. With a maximum maxillary height shared between the lacrimal–jugal and jugal–squamosal contact positions, NHMD 1201206 matches the condition in the type series of *E. wangsjoii* specimens. The dermatocranial ornament also appears similar. What does set the condition in NHMD 1201206 apart from that of *E. wangsjoii* is the tall unornamented zone of overlap that runs along the entire preserved length of the bone (which includes all but the caudal tip). This includes the region that would be overlapped by the squamosal (a region labelled 'od.Sq' by Jarvik 1952, fig. 37c, presumably abbreviating 'area of maxilla overlapped by squamosal' but not listed in the Abbreviations section). Lacrimal and jugal overlap onto maxilla is expected for a tristichopterid, but squamosal overlap onto maxilla is rare (only three species exhibit the condition; see section 4.4) and is counter to the condition observed in the one relevant cheek skeleton in the *E. wangsjoii* type series (NHMD 1201204).

**6.2.5. Palatal bones.** NHMD 142055 (Fig. 18a) from Sederholm Bjerg and NHMD 154652 from Smith Woodward Bjerg both preserve left entopterygoids primarily in visceral impression. The two are similarly sized and shaped to one another and to that of *E. wangsjoii*, with a maximum height in the rostral half of the bone in the position of the dorsal process. Both shallow rostrally and caudally from the dorsal process, but more abruptly in the rostral direction along a concave dorsal margin. Caudal to the process, the dorsal margin is convex in NHMD 142055, like that of *E. wangsjoii*, and is concave in NHMD 154652.

**6.2.6. Lower jaws.** NHMD 141999 from Smith Woodward Bjerg includes potential articulated infradentaries in association with the postparietal shield that shares this catalogue number and is described above. The potential infradentaries are preserved in visceral view and do not offer describable anatomy. NHMD 142054 from Sederholm Bjerg is a dermal impression of the labial surface of a short section of a left lower jaw including part of the dentary and two infradentaries. The dermal ornament in this specimen comprises primarily anastomosing ridges but with tubercles close to the bone margins.

NHMD 153050 (Fig. 18b) is a latex cast of a right lower jaw mould discovered at the same locality as the *E. wangsjoii* holotype on Sederholm Bjerg. The specimen preserves the dentary and coronoid bones in lingual view. There is a dentary fang pair

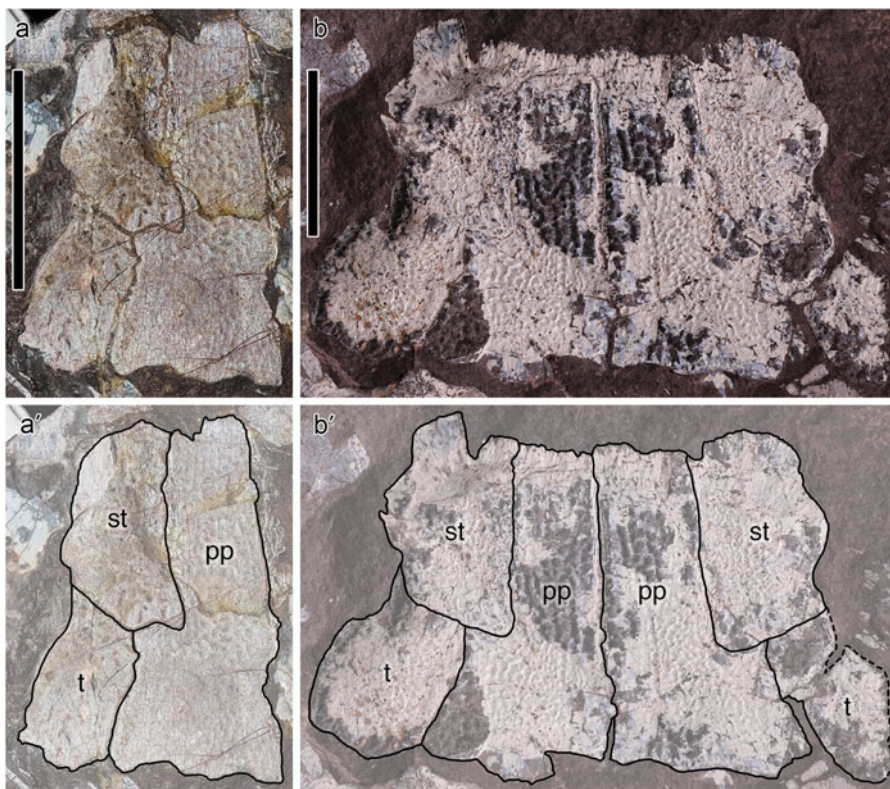


**Figure 16** cf. *E. wangsjoii*: (a) NHMD 141750, left postparietal shield in dermal view (a, photograph; a', labelled illustration); (b) NHMD 141999, postparietal shield primarily in dermal impression (b, photograph; b', labelled illustration). Dashed lines follow unfinished bone margins. Abbreviations: pp = postparietal; st = supratemporal; t = tabular. Scale bars equal 3 cm.

and the marginal row of dentition terminates at the distal dentary fang position and therefore does not reach the symphysis. A short vertical labial lamina of the first and second coronoids does not carry any marginal coronoid dentition. Coronoid 3 is incomplete distally so there is no ability to address the potential for a second fang pair or for marginal dentition on the bone. NHMD 154694 from Sederholm Bjerg is a partial left lower jaw preserving part

of the dentary and fragments of the articulated infradentaries in dermal view; enough of the coronoids are preserved to determine that the first two carry a single fang pair and the third carries two. The dentary decreases in height mesial to distal and a dentary fang pair is confirmed to be present. The dermal surface of the dentary and infradentaries is weathered, but what is visible of the dermal ornament is consistent with the condition in

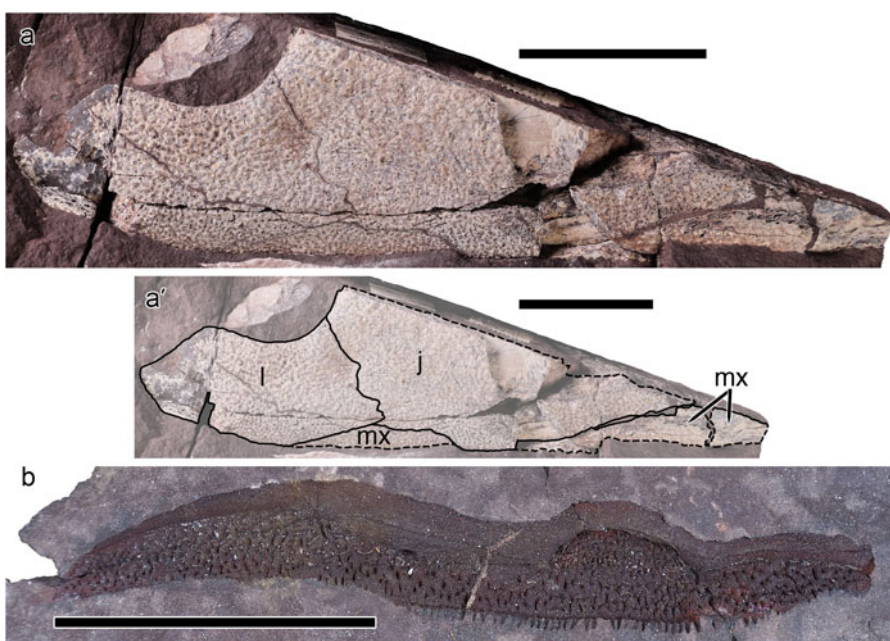


**Figure 17** cf. *E. wangsjoii*: (a) NHMD 141669, partial left cheek in dermal view (a, photograph; a', labelled illustration); (b) NHMD 1201206, left maxilla in dermal impression. Dashed lines follow unfinished bone margins. The surrounding rock matrix of (b) was brightened to accentuate margins of the bone impression. Abbreviations: j = jugal; l = lacrimal; mx = maxilla. Scale bars equal 5 cm.

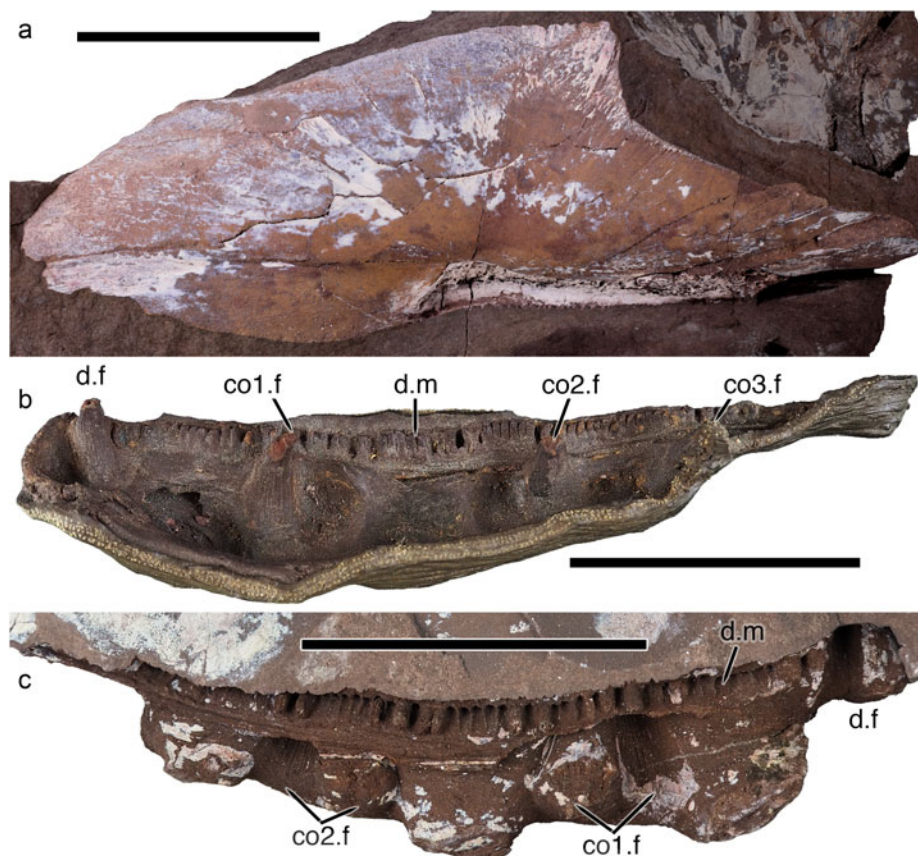


**Figure 18** cf. *E. wangsjoii*: (a) NHMD 142055, left entopterygoid primarily in visceral impression; (b) NHMD 153050, latex cast of partial right lower jaw in lingual view; (c) NHMD 1201219, partial right lower jaw in lingual impression. The surrounding rock matrix of (a) was darkened, and that of (c) was brightened, to accentuate margins of the bone impressions. Abbreviations: co1.f = coronoid 1 fang; co2.f = coronoid 2 fang; co3.f = coronoid 3 fang; d.f = dentary fang; d.m = dentary marginal teeth. Scale bars equal 5 cm.

*E. wangsjoii*. NHMD 154716 from Smith Woodward Bjerg is a dermal impression of the labial surface of a short section of a right lower jaw, including partial dentary and infradentaries. The dermal ornament is consistent with the condition in the *E. wangsjoii* skull.

NHMD 1201219 (Fig. 18c) from an unspecified locality of East Greenland is an impression of a short section of a right dentary (lingual surface) with associated coronoids 1 and 2. There is a dentary fang pair and the bone's marginal tooth row does not appear to continue past the fangs. The first coronoid, at least, carries a short vertical labial lamina that appears to be devoid of marginal coronoid dentition.

**6.2.7. Operculogular/extrascapular series.** NHMD 154434 (Fig. 19a) from lower Stensiö Bjerg on Gauss Halvø is a left opercular preserved in dermal view. The somewhat crescent shape recalls the opercular of NHMD 141653 and the ornament is also similar.

**6.2.8. Pectoral appendicular bones.** NHMD 154652 from Smith Woodward Bjerg includes a visceral impression of a potential anocleithrum, as identified by the crescent shape (concave cranial) and the pointed process of the cranial margin that is expected to be overlapped by the cleithrum.

NHMD 142411 (Fig. 19b) from lower Stensiö Bjerg is a left cleithrum preserved primarily in dermal impression. It is of the typical boomerang shape with a longer dorsal lamina than ventral lamina. It does not have the protruding caudoventral corner that gives the cleithrum of *E. wangsjoii* a heeled appearance nor does it have the long ventral process that has been described for several highly nested tristichopterids including *Hyneria lindae* (Daeschler & Downs 2018) and *Eusthenodon bourdoni* (Downs *et al.* 2021). The dermal ornament of this cleithrum,

unknown in *E. wangsjoii*, comprises anastomosing ridges that are primarily longitudinally oriented. NHMD 154653 (Fig. 19c) from Smith Woodward Bjerg is a right cleithrum in visceral view, though weathered enough to see through to the dermal ornament (similar in texture to that of NHMD 142411 and finer along the cranial margin than along the caudal). This cleithrum is larger than NHMD 142411, has a longer ventral process, and more of a heeled appearance. NHMD 1201212 from Sederholm Bjerg is a fragment of a large left cleithrum's dorsal lamina preserved in dermal view. The ornament is consistent with that of both NHMD 142411 and 1201212.

NHMD 1201221 (P. 1648 of Jarvik 1985; Fig. 19d) from Sederholm Bjerg is a dermal impression of a left clavicle briefly described and assigned to *E. wangsjoii* by Jarvik (1985). The clavicle bone is not represented among the specimens in the type series so no comparison is possible. This specimen shows the dorsal clavicular process and a complex reticulating dermal ornament that is finer along the cranial and lateral margins than it is elsewhere on the bone.

**6.2.9. Summary.** This inventory of cf. *E. wangsjoii* specimens at the NHMD begins to communicate the potential wealth of available specimens that may continue to improve understanding of *E. wangsjoii* and, more generally, highly nested tristichopterids. Owing to a history of reporting that extends back to 1952, *E. wangsjoii* has long served as a model of derived tristichopterid anatomy and has done so even without a sufficient diagnosis or a complete description. The remarkable materials at the NHMD have always suggested greater potential for the species than Jarvik (1952) was able to communicate due to the historical context of that original work. In recent years, my intention has been to elevate *E. wangsjoii* to meet this potential. The present work

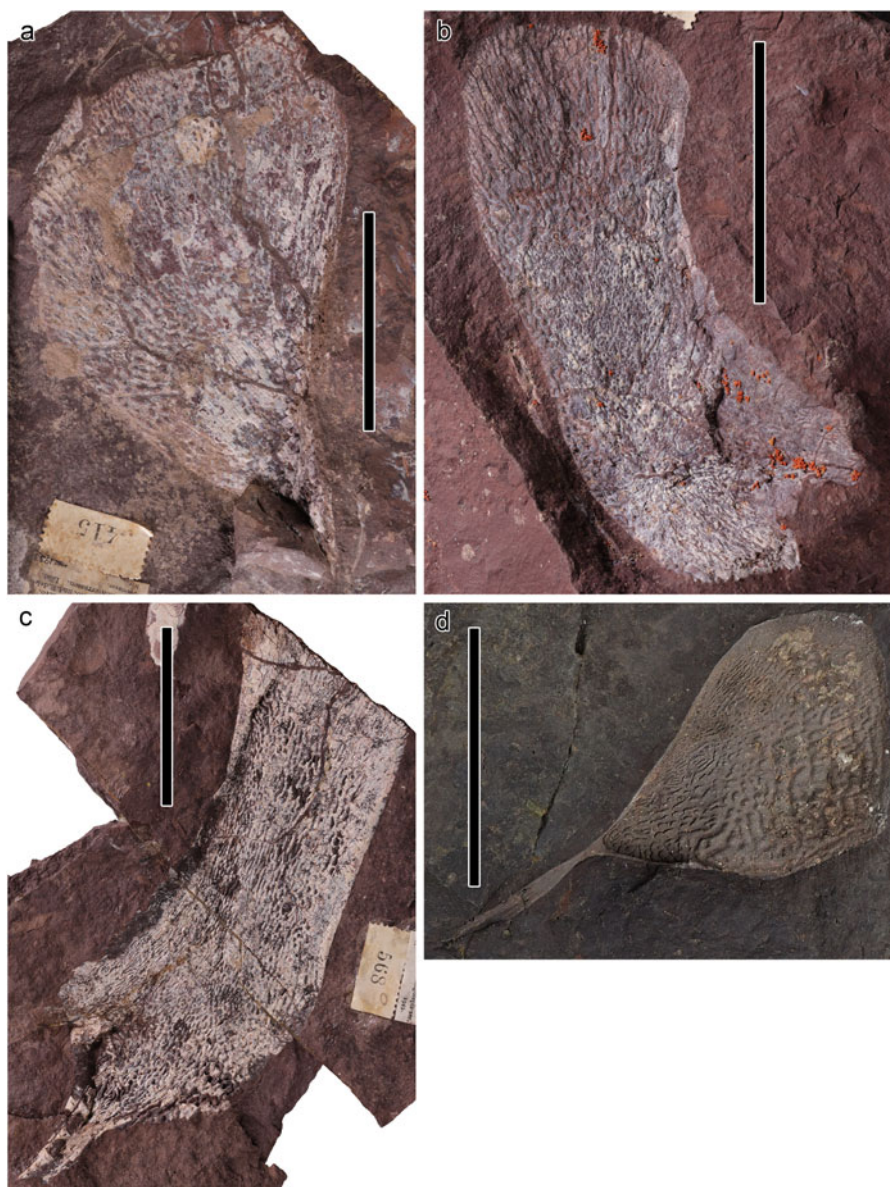


**Figure 19** cf. *E. wangsjoi*: (a) NHMD 154434, left opercular primarily in dermal impression; (b) NHMD 142411, left cleithrum primarily in dermal impression; (c) NHMD 154653, right cleithrum in weathered visceral view; (d) NHMD 1201221, left clavicle in dermal impression. The surrounding rock matrix of (d) was darkened to accentuate margins of the bone impression. Scale bars equal 5 cm.

offers new diagnoses for *Eusthenodon* and its type species (section 3), a comparative description (section 4), phylogenetic results that reflect revised character data for *E. wangsjoi* (section 5), an inventory of potentially relevant specimens in the NHMD collections (section 6.2) and figures that offer the first unobscured look at the *E. wangsjoi* type series of specimens. This work joins the recent descriptions of *Eusthenodon bourdoni* and *Eusthenodon leganihanne* and the taxonomic reports that accompany them: a complete history of *Eusthenodon* diagnoses (Downs *et al.* 2021) and a reconsideration of all historical reports of the taxon's occurrence (Downs *et al.* 2023). Improving the taxonomic status of *E. wangsjoi* may provide the groundwork needed to make new discoveries on other highly nested tristichopterid species, thus bringing even greater clarity to this rapidly expanding part of the tristichopterid lineage.

## 7. Supplementary material

Supplementary material is available online at <https://doi.org/10.1017/S1755691025000015>.

## 8. Acknowledgements

B. Lindow was a remarkable partner during my time in the NHMD collections; I thank him for collections access, his investigations into the collections history of the described materials, and assistance with photography. I thank P. Ahlberg, L. Cotton, E. Daeschler, E. Gilmore and T. Mörs for collections access and/or helpful input. Two anonymous reviewers provided valuable comments that improved the manuscript. This work was made possible by a sabbatical leave granted by Delaware Valley University and the financial support of an anonymous donor.

## 9. Data availability statement

The data that support the findings of this study are openly available at MorphoBank at <http://morphobank.org/permalink/P5678>, project number 5678.

## 10. Competing interests

None.

## 11. References

- Ahlberg, P. E. & Johanson, Z. 1997. Second tristichopterid (Sarcopterygii, Osteolepiformes) from the Upper Devonian of Canowindra, New South Wales, Australia, and phylogeny of the Tristichopteridae. *Journal of Vertebrate Paleontology* **17**, 653–73.
- Ahlberg, P. E. & Johanson, Z. 1998. Osteolepiformes and the ancestry of tetrapods. *Nature* **395**, 792–94.
- Ahlberg, P. E., Johanson, Z. & Daeschler, E. B. 2001. The Late Devonian *Soederberghia* (Sarcopterygii, Dipnoi) from Australia and North America, and its biogeographical implications. *Journal of Vertebrate Paleontology* **21**, 1–12.
- Anderson, M. E., Long, J. A., Evans, F. J., Almond, J. E., Theron, J. N. & Bender, P. A. 1999. Biogeographic affinities of Middle and Late Devonian fishes of South Africa. *Records of the Western Australian Museum Supplement* **57**, 157–68.
- Berg, L. S. 1937. A classification of fish-like vertebrates. *Bulletin of the Academy of Sciences of the USSR* **4**, 1277–80.
- Blom, H., Clack, J. A., Ahlberg, P. E. & Friedman, M. 2007. Devonian vertebrates from East Greenland: a review of faunal composition and distribution. *Geodiversitas* **29**, 119–41.
- Borgen, U. J. & Nakrem, H. A. 2016. Morphology, phylogeny and taxonomy of osteolepiform fish. *Fossil and Strata* **61**, 1–514.
- Clément, G. 2002. Large Tristichopteridae (Sarcopterygii; Tetrapodomorpha) from the late Famennian Evieux Formation of Belgium. *Palaeontology* **45**, 577–93.
- Clément, G., Snitting, D. & Ahlberg, P. E. 2009. A new tristichopterid (Sarcopterygii, Tetrapodomorpha) from the Upper Famennian Evieux Formation (Upper Devonian) of Belgium. *Palaeontology* **52**, 823–36.
- Cope, E. D. 1889. Synopsis of the families of Vertebrata. *American Naturalist* **23**, 843–77.
- Daeschler, E. B. & Downs, J. P. 2018. New description and diagnosis of *Hyneria lindae* (Sarcopterygii, Tristichopteridae) from the Upper Devonian Catskill Formation in Pennsylvania, USA. *Journal of Vertebrate Paleontology* **38**, e1448834. doi: 10.1080/02724634.2018.1448834.
- Daeschler, E. B., Downs, J. P. & Matzko, C. 2019. New material supports a description and taxonomic revision of *Holoptychius ? radiatus* (Sarcopterygii, Tristichopteridae) from the Upper Devonian Catskill Formation in Pennsylvania, USA. *Proceedings of the Academy of Natural Sciences of Philadelphia* **167**, 11–25.
- de Queiroz, K. & Cantino, P. D. 2020. *International code of phylogenetic nomenclature (PhyloCode)*. Boca Raton: CRC Press, 190 pp.
- Downs, J. P., Barbosa, J. & Daeschler, E. B. 2021. A new species of *Eusthenodon* (Sarcopterygii, Tristichopteridae) from the Upper Devonian (Famennian) of Pennsylvania, USA, and a review of *Eusthenodon* taxonomy. *Journal of Vertebrate Paleontology* **41**, e1976197. doi: 10.1080/02724634.2021.1976197.
- Downs, J. P. & Daeschler, E. B. 2022. Second species of *Langleria* (Tristichopteridae, Sarcopterygii) from the Upper Devonian Catskill Formation of Pennsylvania, USA, and a new phylogenetic consideration of Tristichopteridae. *Proceedings of the Academy of Natural Sciences of Philadelphia* **167**, 241–60.
- Downs, J. P., Long, A., Daeschler, E. B. & Shubin, N. H. 2018. *Eusthenopteron jenkinsi* sp. nov. (Sarcopterygii, Tristichopteridae) from the Upper Devonian of Nunavut, Canada, and a review of *Eusthenopteron* taxonomy. *Breviora* **562**, 1–24.
- Downs, J. P., Osatchuck, M. M., Goodchild, O. A. & Daeschler, E. B. 2023. Second species of *Eusthenodon* (Tristichopteridae, Sarcopterygii) from the Upper Devonian (Famennian) Catskill Formation of Pennsylvania, USA, and a review of global *Eusthenodon* occurrence. *Journal of Vertebrate Paleontology* **42**, e2201627. doi: 10.1080/02724634.2023.2201627.
- Egerton, P. M. G. 1861. *Tristichopterus alatus*. *Memoirs of the Geological Survey of the United Kingdom* **10**, 51–55.
- Gess, R. W. & Ahlberg, P. E. 2023. A high latitude Gondwanan species of the Late Devonian tristichopterid *Hyneria* (Osteichthyes: Sarcopterygii). *PLoS ONE* **18**, e0281333.
- Jarvik, E. 1944. On the dermal bones, sensory canals and pitlines of the skull in *Eusthenopteron foordi* Whiteaves, with some remarks on *E. säve-söderberghi* Jarvik. *Kungliga Svenska Vetenskapsakademiens Handlingar* **21**, 1–48.
- Jarvik, E. 1952. On the fish-like tail in the ichthyostegid stegocephalians with descriptions of a new stegocephalian and a new crossopterygian from the Upper Devonian of East Greenland. *Meddelelser om Grønland* **114**, 1–90.
- Jarvik, E. 1980. *Basic structure and evolution of vertebrates* Vol. 1. London: Academic Press.
- Jarvik, E. 1985. Devonian osteolepiform fishes from East Greenland. *Meddelelser om Grønland, Geoscience* **13**, 1–52.
- Jarvik, E. 1996. The Devonian tetrapod *Ichthyostega*. *Fossils and Strata* **40**, 1–213.
- Johanson, Z. 2004. Late Devonian sarcopterygian fishes from eastern Gondwana (Australia and Antarctica) and their importance in phylogeny and biogeography. In Arratia, G., Wilson, M. V. H. & Cloutier, R. (eds) *Recent advances in the origin and early radiation of vertebrates*, 287–308. Munich: Verlag Dr Friedrich Pfeil.
- Johanson, Z. & Ahlberg, P. E. 1997. A new tristichopterid (Osteolepiformes: Sarcopterygii) from the Mandagery Sandstone (Late Devonian, Famennian) near Canowindra, NSW, Australia. *Transactions of the Royal Society of Edinburgh, Earth Sciences* **88**, 39–68.
- Johanson, Z. & Ahlberg, P. E. 2001. Devonian rhizodontids and tristichopterids (Sarcopterygii; Tetrapodomorpha) from east Gondwana. *Transactions of the Royal Society of Edinburgh, Earth Sciences* **92**, 43–74.
- Johanson, Z. & Ritchie, A. 2000. Rhipidistians (Sarcopterygii) from the Hunter Siltstone (Late Famennian) near Grenfell, NSW, Australia. *Mitteilungen aus dem Museum für Naturkunde in Berlin, Geowissenschaftliche Reihe* **3**, 111–36.
- Lebedev, O. 1992. The latest Devonian, Khovanian vertebrate assemblage of Andreyevka-2 locality, Tula Region, Russia. In Mark-Kurik, E. (ed.) *Fossil fishes as living animals, proceedings of the II International Colloquium on the Study of the Palaeozoic Fishes, Tallinn, 1989, Academia* Vol. **1**, 265–72. Tallinn: Institute of Geology of the Estonian Academy of Sciences.
- Lehman, H. P. 1959. Les dipneustes du Dévonien supérieur du Groenland [The Upper Devonian lungfish of Greenland]. *Meddelelser om Grønland* **160**, 1–58.
- Maddison, W. & Maddison, D. 2021. Mesquite: a modular system for evolutionary analysis (version 3.70, build 940). <https://www.mesquiteproject.org>.
- Newberry, J. S. 1889. *The paleozoic fishes of North America*. Reston: US Geological Survey.
- Olive, S., Leroy, Y., Daeschler, E. B., Downs, J. P., Ladevèze, S. & Clément, G. 2020. Tristichopterids (Sarcopterygii, Tetrapodomorpha) from the Upper Devonian tetrapod-bearing locality of Strud (Belgium, Upper Famennian), with phylogenetic and paleobiogeographic considerations. *Journal of Vertebrate Paleontology* **40**, e1768105. doi: 10.1080/02724634.2020.1768105.
- Olsen, H. & Larsen, P.-H. 1993. Lithostratigraphy of the continental Devonian sediments in north-east Greenland. *Bulletin Grønlands Geologiske Undersøgelse* **165**, 1–108.
- Romer, A. S. 1955. Herpetichthyes, Amphibioidei, Choanichthyes or Sarcopterygii? *Nature* **176**, 126.
- Säve-Söderbergh, G. 1932. Preliminary note on Devonian stegocephalians from East Greenland. *Meddelelser om Grønland* **94**, 1–105.
- Säve-Söderbergh, G. 1933. Further contributions to the Devonian stratigraphy of East Greenland I: results from the summer expedition 1932. *Meddelelser om Grønland* **96**, 1–52.
- Säve-Söderbergh, G. 1934. Further contributions to the Devonian stratigraphy of East Greenland II: investigations on Gauss Peninsula during the summer of 1933. With an appendix: notes on the geology of the Passage Hills (East Greenland). *Meddelelser om Grønland* **96**, 1–74.
- Snitting, D. 2008. Morphology, taxonomy, and interrelationships of tristichopterid fishes (Sarcopterygii, Tetrapodomorpha). *Digital Comprehensive Summaries of Uppsala Dissertations from the Faculty of Science and Technology* **421**, 1–195.
- Snitting, D. 2009. *Heddeleithys* – a new tristichopterid genus from the Dura Den Formation, Midland Valley, Scotland (Famennian, Late Devonian). *Acta Zoologica* **90** (1, supplement), 273–84.
- Stensiö, E. 1931. Upper Devonian vertebrates from East Greenland. *Meddelelser om Grønland* **86**, 1–212.
- Swartz, B. 2012. A marine stem-tetrapod from the Devonian of western North America. *PLoS ONE* **7**, e33683.
- Swofford, D. L. 2002. PAUP\*: phylogenetic analysis using parsimony (and other methods): version 4.0a62. <http://phylosolutions.com>.
- Thomson, K. S. 1976. The faunal relationships of rhipidistian fishes (Crossopterygii) from the Catskill (Upper Devonian) of Pennsylvania. *Journal of Paleontology* **50**, 1203–08.
- Vorobyeva, E. I. 1960. O sistematicheskoy polozhenii *Eusthenopteron wenjukowi* (Rohon) [On the systematic position of *Eusthenopteron wenjukowi* (Rohon)]. *Palaeontologicheskii Zhurnal* **2**, 121–29.
- Vorobyeva, E. I. 1962. Rhizodontnye kisteperyye ryby Glavnogo devonskogo polya SSSR [Rhizodontid crossopterygians of the main Devonian field of the USSR]. *Trudy Paleontologicheskogo Instituta, Akademia Nauk SSSR* **94**, 1–140.
- Vorobyeva, E. I. 1977. Morfologiya i osobennosti evolyutsii kisteperykh ryb [Morphology and features of the evolution of crossopterygian

- fishes]. *Trudy Paleontologicheskogo Instituta Akademia Nauk SSSR* **163**, 1–240.
- Whiteaves, J. F. 1881. On some remarkable fossil fishes from the Devonian rocks of Scaumenac Bay, in the Province of Quebec. *American Journal of Science* **21**, 494–96 [reprinted in *Annals and Magazine of Natural History* **8**, 159–62].
- Woodward, A. S. 1900. Notes on some Upper Devonian fish-remains, discovered by Prof A. G. Nathorst in East Greenland. *Bihang till Kungliga Svenska Vetenskapsakademiens Handlingar* **26**, 1–10.
- Young, G. C. 1993. Middle Palaeozoic macrovertebrate biostratigraphy of eastern Gondwana. In Long, J. A. (ed.) *Palaeozoic vertebrate biostratigraphy and biogeography*, 208–51. Baltimore: The Johns Hopkins University Press.
- Young, G. C. 2008. Relationships of tristichopterids (osteolepiform lobe-finned fishes) from the Middle–Late Devonian of east Gondwana. *Alcheringa: An Australasian Journal of Palaeontology* **32**, 321–36.
- Young, G. C., Dunstone, R. L., Ollerenshaw, P. J., Lu, J. & Crook, B. 2019. New information on the giant Devonian lobe-finned fish *Ede-nopteron* from the New South Wales coast. *Australian Journal of Earth Sciences* **67**, 221–42. doi: 10.1080/08120099.2019.1651769.
- Young, B., Dunstone, R. L., Senden, T. J. & Young, G. C. 2013. A gigantic sarcopterygian (tetrapodomorph lobe-finned fish) from the Upper Devonian of Gondwana (Eden, New South Wales, Australia). *PLoS ONE* **8**, e53871.
- Zhu, M. & Ahlberg, P. E. 2004. The origin of the internal nostril of tetrapods. *Nature* **432**, 94–97.

---

MS received 15 November 2024. Accepted for publication 18 February 2025